University of Zurich[UZH]

Zurich Open Repository and Archive
University of Zurich
University Library
Strickhofstrasse 39
CH-8057 Zurich
www.zora.uzh.ch

Year: 2016

Rat intra-hippocampal NMDA infusion induces cell-specific damage and changes in expression of NMDA and GABAA receptor subunits

Rambousek, Lukas ; Kleteckova, Lenka ; Kubesova, Anna ; Jirak, Daniel ; Vales, Karel ; Fritschy, Jean-Marc

Abstract: Excessive stimulation of NMDA receptors with glutamate or other potent agonists such as NMDA leads to excitotoxicity and neural injury. In this study, we aimed to provide insight into an animal model of brain excitotoxic damage; single unilateral infusion of NMDA at mild dose into the hippocampal formation. NMDA infusion induced chronic, focal neurodegeneration in the proximity of the injection site. The lesion was accompanied by severe and progressive neuroinflammation and affected preferentially principal neurons while sparing GABAergic interneurons. Furthermore, the unilateral lesion did not cause significant impairment of spatial learning abilities. Finally, GluN1 and GluN2B subunits of NMDA receptor were significantly upregulated up to 3 days after the NMDA infusion, while GABAA 5 subunit was downregulated at 30 days after the lesion. Taken together, a single infusion of NMDA into the hippocampal formation represents an animal model of excitotoxicity-induced chronic neurodegeneration of principal neurons accompanied by severe neuroinflammation and subunit specific changes in NMDA and GABAA receptors.

DOI: https://doi.org/10.1016/j.neuropharm.2016.02.035

Posted at the Zurich Open Repository and Archive, University of Zurich
ZORA URL: https://doi.org/10.5167/uzh-131546
Journal Article
Accepted Version

The following work is licensed under a Creative Commons: Attribution-NonCommercial-NoDerivatives 4.0 International (CC BY-NC-ND 4.0) License.

Originally published at:
Rambousek, Lukas; Kleteckova, Lenka; Kubesova, Anna; Jirak, Daniel; Vales, Karel; Fritschy, Jean-Marc (2016). Rat intra-hippocampal NMDA infusion induces cell-specific damage and changes in expression of NMDA and GABAA receptor subunits. Neuropharmacology, 105:594-606.
DOI: https://doi.org/10.1016/j.neuropharm.2016.02.035

Rat intra-hippocampal NMDA infusion induces cell-specific damage and changes in expression of NMDA and $GABA_A$ receptor subunits

Rambousek Lukas[1, 2, 3], Kleteckova Lenka[2, 3], Kubesova Anna[4], Jirak Daniel[5, 6], Vales Karel[3, 4], Fritschy Jean-Marc[1, 7]

1. Neuromorphology Group, Institute of Pharmacology and Toxicology, University of Zurich, Zurich, Switzerland
2. 2nd Faculty of Medicine, Charles University, Prague, Czech Republic
3. Institute of Physiology, Academy of Sciences, Prague, Czech Republic
4. National Institute of Mental Health, Klecany, Czech Republic
5. Institute for Clinical and Experimental Medicine, Prague, Czech Republic
6. Institute of Biophysics and Informatics, 1st Medicine Faculty, Charles University, Prague, Czech Republic
7. Neuroscience Center Zurich, University and ETH Zurich, Zurich, Switzerland

Corresponding author:

Lukas Rambousek, Ph.D.
University of Zurich, Institute of Experimental Immunology, Winterthurerstrasse 190, Zurich Switzerland
rambousek@immunology.uzh.ch

Highlights:

1. The infusion of NMDA induced degeneration of hippocampal principal cells.
2. Neurodegeneration was accompanied with progressive and severe neuroinflammation.
3. The lesion did not induce loss of GABAergic interneurons.
4. GluN1 and GluN2B subunits of NMDA receptor were upregulated at early time points.
5. $GABA_A$ receptor α5 subunit was downregulated at 30 days after the lesion.

ABSTRACT

Excessive stimulation of NMDA receptors with glutamate or other potent agonists such as NMDA leads to excitotoxicity and neural injury. In this study, we aimed to provide insight into an animal model of brain excitotoxic damage; single unilateral infusion of NMDA at mild dose into the hippocampal formation. NMDA infusion induced chronic, focal neurodegeneration in the proximity of the injection site. The lesion was accompanied by severe and progressive neuroinflammation and affected preferentially principal neurons while sparing GABAergic interneurons. Furthermore, the unilateral lesion did not cause significant impairment of spatial learning abilities. Finally, GluN1 and GluN2B subunits of NMDA receptor were significantly upregulated up to 3 days after the NMDA infusion, while $GABA_A$ α5 subunit was downregulated at 30 days after the lesion. Taken together, a single infusion of NMDA into the hippocampal formation represents an animal model of excitotoxicity-induced chronic neurodegeneration of principal neurons accompanied by severe neuroinflammation and subunit specific changes in NMDA and $GABA_A$ receptors.

1. INTRODUCTION

N-methyl-D-aspartate (NMDA) receptors are a sub-family of glutamate-gated ion channels, the most abundant receptors in mammalian brain responsible for mediating excitatory neurotransmission. They are blocked with Mg^{2+} at membrane potential, require co-activation by glutamate and glycine (or D-serine) and are a major gate for Ca^{2+}-induced postsynaptic signaling. Native NMDA receptors consist of two GluN1 and either two GluN2 or GluN3 subunits. The GluN1 subunit is necessary for the assembly of functional NMDA receptors (Zukin and Bennett, 1995). Furthermore, the receptor can have many isoforms (GluN1 has 8 different splice variants, GluN2A, B, C, D; GluN3A, B) with diverse brain localization and function (Sheng and Kim, 2002). NMDA receptors are important in brain development, generation of rhythms, neural plasticity, memory, learning and neuroprotection (Paoletti and Neyton, 2007; Cull-Candy et al., 2001).

Excessive stimulation of NMDA receptors with glutamate or other potent agonists such as NMDA leads to excitotoxicity (Sattler and Tymianski, 2001). This process is characterized by massive depolarization of postsynaptic membrane, leading to influx of water, Na^+ and Cl^- ions, osmotic imbalance and possible breakdown of the cell. Excitotoxicity also increases intracellular calcium levels leading to enhanced free radical formation, activation of phospholipases, endonucleases and proteases and subsequent cell damage or death. Excitotoxicity occurs in a number of pathological conditions such as stroke and ischemia (Lai et al., 2014), traumatic brain injury (Caccamo et al., 2004), as well as neurodegenerative diseases (Mehta et al., 2013).

Infusion of NMDA into the brain parenchyma has been utilized as an animal model of excitotoxicity to induce structure-specific damage of nervous tissue (White et al., 2003; Wallace and Whishaw, 2003, Maren et al., 1997 1999). This approach has also been used extensively by behavioral neuroscientists to study the role of different brain regions in cognitive processing; especially, the role of hippocampus in learning and memory (Kim and Frank, 2009; Dillon at al., 2008; Maren et al., 1997; Sparks et al., 2011). Additionally, this model has been utilized to induce chronic neuroinflammation (Battle et al., 2015) and to test the efficacy of neuroprotective drugs (Rambousek et al., 2011). Furthermore, systemic administration of NMDA has been utilized to elicite epileptic motor seizures in developing as well as in young adult rats (Mares and Velisek, 1992).

It is well described that NMDA infusion into the hippocampal formation induces loss of pyramidal cells and dentate gyrus granule cells (Jarrard, 2002). The extent and severity of the hippocampal lesion depends on the dose and the number of injections. With very low doses, it is possible to induce damage of a few neurons in focal area whereas high doses are able to lesion a large amount of tissue (White et al., 2003; Wallace and Whishaw, 2003). Intra-hippocampal infusion of NMDA also induces severe seizures during the hours after application (Zaczek and Coyle, 1981) in adult rats. However, to our knowledge there is no report investigating the effect of hippocampal NMDA lesions in adult animals on seizure activity on a longer time axis.

The changes induced by NMDA infusion, such as expression of NMDA and $GABA_A$ receptors subunits or cell-specific injury, have received little attention so far. Therefore, we aimed to further characterize this model of excitotoxic damage in adult rats. We characterized immunohistochemically the changes induced by unilateral infusion of 1 µL of 25 mM NMDA into the hippocampus at 1, 3, 7 and 30 days post-injection (dpi). First, we determined the effect of NMDA on neuronal degeneration and spatial learning abilities. Then, we characterized the temporal progression of neuroinflammation using antibodies against microglial marker Iba-1 and astrocytic marker glial fibrillary acidic protein (GFAP). Since previous reports hypothesized that GABAergic interneurons tolerate excitotoxic insults (Avigone et al., 2005), we evaluated effect of NMDA lesion also on populations of interneurons expressing the calcium binding proteins parvalbumin, calretinin, calbindin, as well as the neuropeptide Y (NPY). Finally, we investigated immunohistochemically the temporal progression of changes in expression of major NMDA (GluN1, GluN2B) and $GABA_A$ (α1, α2, α5 and γ2) receptor subunits. We show that NMDA infusion induces long-lasting degeneration of glutamatergic neurons leaving GABAergic interneurons unaffected and causes subunit-specific changes in expression of NMDA and $GABA_A$ receptors.

2. METHODS

Animals and intra-hippocampal NMDA infusion

We utilized three months old male Long-Evans rats from the breeding colony of Institute of Physiology of the Academy of Sciences of the Czech Republic (CZ 11760353). All animals were anaesthetized with isoflurane 3.5% (Abbot Laboratories, UK) in a specialized induction chamber. During surgery, animals were fixed using a stereotactic apparatus (TSE systems, Germany) and anaesthetized with isoflurane 1.5 - 2%, propelled by atmospheric air. Small opening in the skull was made using a micro-drill (Dremel, USA) and subsequently 1 μL of 25 mM NMDA (Sigma Aldrich, Germany) or 10 mM of sterile PBS (sham group; Sigma Aldrich, USA) was applied unilaterally at a flow rate of 0.2 μL/min into the dorsal left hippocampus with a pump (TSE, model 540310 plus) and 2 min after the end of infusion the needle (#7635-01, Hamilton) was retracted. To prevent the loss of tissue integrity that was reported in previous studies (White et al., 2003; Wallace and Whishaw, 2003), we utilized mild (25 mM) concentration of NMDA in this experiment. The application coordinates (−4 mm AP from bregma, +2.5 mm ML and 4.8 mm below the skull surface) were measured in relation to a stereotaxic atlas (Paxinos and Watson, 1998). For the evaluation of spatial learning abilities of rats we used also higher dose of NMDA (50 mM) and bilateral infusion.

The NMDA (#M3262, Sigma Aldrich, USA) working solution was prepared in 10 mM PBS (Sigma Aldrich, USA), pH adjusted to 7.4, fractioned in a small volume aliquots (20 μL) and stored at -20 °C. A fresh aliquot from the same batch was used for all experiments. Each aliquot was used only once.

Three animals were used for magnetic resonance imaging. Seven to ten animals per group, 44 in total, were used for behavioral experiment (Carousel maze). Five animals per group were used [SHAM and NMDA lesion group x 1, 3, 7 and 30 dpi; 40 in total] for histology experiments. In total, we utilized 87 experimental animals in this study. All experimental procedures complied with the Animal Protection Code of the Czech Republic, the appropriate directive of the European Union (2010/63/EC) and NIH guidelines.

Magnetic resonance (MR) imaging

MR imaging of animals under general anesthesia (isoflurane 2%) was performed using a 4.7-T Bruker spectrometer equipped with a resonator coil. Animals were imaged one day before the

lesion and then 1, 3, and 7 days after the intra-hippocampal NMDA infusion. A T_2-weighted turbospin echo sequence Rapid Acquisition with Relaxation Enhancement [RARE; repetition time (TR) = 3,000 ms, effective echo time (TE) = 36.0 ms, turbo factor = 8, number of acquisitions (AC) = 4, field of view = 3.5 cm, matrix = 256 × 256, spatial resolution = 137 × 137 μm^2, slice thickness = 0.85 mm, acquisition time = 4 min] was used for measurement of axial and coronal images.

Evaluation of spatial learning abilities – Carousel Maze

The Carousel maze apparatus was described in detail in our previous studies (Stuchlik et al., 2004, 2013, 2014). Briefly, experimental animals have to avoid to shock sector on rotating circular arena. The sector where rats receive mild electric shock is not marked on the arena, thus animal have to utilize visual cues in experimental room to learn its position. In other words, animals have to choose allothetic strategy in order to successfully solve the task. The number of entrances into the to-be-avoided sector (number of errors) measures the efficiency of avoidance in the Carousel maze. In this experiment, rats were trained for four consecutive days in 20 min long sessions. This training procedure was found to be long enough to induce optimal spatial avoidance of the shock sector and the data from the fourth session represents asymptotic levels of performance. Thus, only data from session four were analyzed. The training of rats in the Carousel maze started 7 days after the infusion of NMDA into hippocampal formation; hence, the fourth session took place at day 11 after surgery.

Histology

At 1, 3, 7 or 30 dpi, rats were anaesthetized with an overdosed mixture of ketamine (Vetoquinol) and xylasine (Alfasan) and transcardially perfused at a flow 50 mL/min with 250 mL, 4 °C, 4% paraformaldehyde (PFA) in 0.1 M PBS, preceded by a 5 min rinse with 0.01 M PBS. After postfixation in the same fixative overnight, the brains were stored in a 1% PFA solution at 4 °C, cryoprotected in 10% and consequently 30 % sucrose solution. Brain tissue was stored at -80°C. Free-floating sections (40 µm thick) were cut coronally on a sliding microtome (Leica), and 18 random sampled serial sections were collected from bregma -1.5 to -6.6 mm and stored at - 20°C in cryoprotective solution.

Fluoro-Jade B staining and scoring of neuronal damage

Fluoro-Jade B dye, the fluorescin derivative, has been utilized to visualize neuronal injury and degeneration (Schmued and Hopkins, 2000). Both the chemical entity of this compound and the target component are not identified. However, its specificity for degenerating neurons has been validated using a number of neurotoxins. The sections were mounted on Superfrost Plus Gold (Thermo) microscope slides and let dry overnight. Then the slides were consequently incubated in 100% ethanol for 3 min, 70% ethanol for 3 min, distilled water for 2 min, 0.06 % $KMnO_4$ for 15 min, distilled water for 2 min, 0.0001 % solution of FJB (Millipore, USA, dissolved in 0.1 % glacial acetic acid) for 30 min and finally rinsed three times in distilled water. The slides wwere air-dried, immersed to xylene and coverslipped with DPX mounting media (Thermo). Brain sections were imaged using a microscope (AxioVision Imaginer Z1; Zeiss, Germany) equipped with a digital camera. Alexa 448 filter was used. Extent of damage was evaluated separately in individual areas of the hippocampal formation, namely CA1, CA3, dentate gyrus, hilus and subiculum. The range of damage was expressed as a percentage of hippocampal area with Fluoro-Jade B positive neurons. Evaluation scale: 0 – 0-5%, 1 – 6-25%, 2 – 26-50%, 3 – 51-75%, 4 > 75% Fluoro-Jade B-positive neurons in individual hippocampal area.

Immunohistochemistry

Immunohistochemistry was performed with one series of brain sections per animal, allowing us to analyze each marker under equal conditions for all animals. The primary antibodies used in the study are listed in Table 1. The free-floating sections were rinsed in Tris-Triton solution (0.05 M Tris, 0.015 NaCl, 0.05 % Triton, pH = 7.4) three times for 10 min, followed by overnight incubation in the primary antibodies diluted in Tris-Triton containing 2% normal goat serum (NGS), 0.2% TritonX-100 at 4°C on a shaker.

Sections used for detecting NMDAR GluN1 and GluN2B subunits were additionally digested by pepsin before incubating in primary antibodies. This procedure significantly improves the detection of membrane proteins (Watanabe et al., 1998). Briefly, the sections were incubated at 37°C for 10 min in 0.2 M HCl solution and consequently for additional 10 min in 0.2 M HCl solution containing 0.15 mg/mL pepsin (Dako, S3002, CA, USA). After washing in PBS for 5 min and twice in Tris-Triton for 10 min the sections were incubated in primary antibodies.

On the second day, the sections were rinsed in three times for 10 min in Tris-Triton, then incubated with biotinylated secondary goat antibodies diluted at 1:300 in Tris-Triton containing 2% normal goat serum (NGS) and 2% rat serum for 30 min at room temperature under continuous agitation. After three washing cycles in PBS the sections were incubated in Elite ABC Kit (Vector Laboratories Inc., California, USA) diluted in PBS, 0.2% TritonX-100 for 1 h, and washed three times for 10 min in Tris-Triton. Secondary antibodies were visualized using 0.05% solution of 3,3-diaminobenzidine (DAB, Fluka, Switzerland) and 0.01 % H_2O_2 in Tris-Triton pH 7.7. A fresh aliquot from same batch was used for each experiment. The color reaction was terminated after 8 min by transferring the sections in ice-cold PBS. To prevent intra-group variation, all sections for each marker were stained in one DAB experiment. After two additional washes in PBS the sections were mounted on gelatine-coated slides, dried overnight, dehydrated and cover slipped with Eukitt^{TM} mounting media (Sigma Aldrich, Germany).

Densitometry

Densitometry measurements of $GABA_A$ and NMDA receptor subunits immunoreactivities were measured using ImageJ software (NIH, Maryland, USA). Digital images were acquired with a 20x objective (NA 0.8 NA air) using a 3-CCD digital color camera (Hitachi HV - F22, 1360 x 1024 pixels, pixel size 4.65 μm) mounted in an automated upright slide scanning microscope, Zeiss Mirax mini slides-canner (Zeiss, Jena, Germany). Acquired images of hippocampus and neocortex were then exported at a 5x magnification using Panoramatic viewer (3DHISTECH, Hungary). The optical density (OD) for each hippocampus was normalized to the optical density of neocortex. The optical density of neocortex did not differ significantly within the groups. Four to six regularly-spaced coronal sections from each animal were analyzed. The optical densities for each hippocampus were averaged per animal using the following formula:

$$OD = \frac{\sum_{i=0}^{n}(OD_{neocortex} - OD_{hippocampus})}{n}$$

where *n* is number of sections and *OD* optical density measured as pixel intensity in a range of 0 – 255 using ImageJ software.

A densitometric segmentation analysis was performed for the anti-GFAP (astroglial marker), and anti-Iba1 (activated microglia marker) immunoperoxidase staining to measure the relative percentage of the labeled cells covered by the immunoreactive signals in the hippocampal formation. The quantification was performed using a developed macro in ImageJ software (NIH, Maryland, USA). The pictures obtained with Zeiss Mirax mini slides-canner were converted to 8-bit images, Gaussian blur filter was applied and the background was subtracted. Next the threshold function was applied and relative percentage of the labeled cells covered by the immunoreactive signal was automatically calculated.

Data were analyzed and statistically compared between groups using two-way ANOVA. Ipsilateral and contralateral hippocampi were analyzed separately. Staining intensities, represented as normalized relative optical densities using 2 x 4 ANOVA design to detect effect of group (NMDA lesion or PBS infusion) and day post-injection. Following the confirmation of main effects, Bonferroni's post-hoc tests were performed. Statistical significance was set at $P < 0.05$.

Hippocampal volume estimation

The volume of hippocampus for each animal was estimated from series of sections from immunohistochemistry experiments. Twenty-two sections were analyzed from -1.6 to -5.8 cm from the bregma. The surface area was measured using ImageJ software (NIH, Maryland, USA). Panoramatic viewer determined the absolute scale and pictures were exported including the scale mark. Then we set the scale using the "set scale function" in ImageJ. Volumes were calculated by multiplying the surface area by the distance between measured sections. Data were analyzed and statistically compared between groups using two-way ANOVA as described in the section „densitometry".

3. RESULTS

Unilateral intra-hippocampal NMDA induced focal neurodegeneration and increase in T_2 signal

In this experiment, we characterized temporal progression of changes induced by unilateral infusion of NMDA into the hippocampal formation. After infusion of NMDA into hippocampal formation, all animals suffered from severe seizures lasting two to four hours after surgery. The lesion induced severe neurodegeneration of principal glutamatergic neurons, pyramidal and granule cells, in dorsal hippocampus and dentate gyrus. The damage of glutamatergic neurons remained focal and presumably reflects the diffusion of the injected NMDA solution. One-day post injection the Fluoro-Jade B signal was most prominent within cell body and later it propagated to axon and dendrites. However, the damage did not spread into the contralateral hemisphere or into the ventral part of ipsilateral hippocampal formation. The lesion also did not propagate to other brain structures. Fig. 1 shows representative pictures of dorsal ipsilateral hippocampal formation 1, 3, 7 and 30 dpi. Sham lesion did not induce neurodegeneration (score 0). Only minor morphological signs of tissue damage in the proximity of cannula were observed. One-way ANOVA did not find significant effect ($P > 0.05$) in progression of damage score in any of studied subfields of hippocampal formation (CA1, CA3, dentate gyrus, hilus and subiculum). Interestingly, the severity of neurodegeneration measured as damage score of FJB positive cells did not change over 30 days. The neurons affected by NMDA were swollen; however, they sustained their basic morphology. Two-way ANOVA also did not find significant changes in hippocampal volume after NMDA infusion [NMDA treatment ($F_{(1, 19)} = 0.002$, $P = 0.9674$), dpi ($F_{(19, 19)} = 0.8457$, $P = 0.6406$)]; however, we observed mild hippocampal sclerosis 30 dpi in two animals from five (Fig. 2). The contralateral hippocampus was not affected at any of study time-points. To further visualize the extent and progression of the lesion in the same animal, we performed MR imaging in three rats. Infusion of NMDA into hippocampus induced an increase in T_2 signal (Fig. 3) in the hippocampal formation at 1 dpi. The signal decreased progressively thereafter; however, it was still detectable at 7 dpi.

Unilateral lesion of hippocampus did not induce a deficit in spatial learning abilities

The one-way ANOVA did not reveal a significant effect of unilateral intra-hippocampal infusion of 25 mM NMDA ($P > 0.05$). Neither a higher dose of 50 mM induced spatial learning deficits in

the Carousel maze ($P > 0.05$). On the other hand, bilateral infusion of NMDA at both doses (25 and 50 mM) induced significant ($P < 0.05$ and $P < 0.005$, respectively) spatial learning deficit measured as number of errors in Carousel Maze. Fig. 4 depicts the number of errors, the parameter reflecting spatial learning abilities of rats in the Carousel maze.

NMDA lesion did not affect GABAergic interneurons

The utilization of specific antibodies against separate populations of GABAergic interneurons revealed that NMDA infusion did not induce any apparent loss in hippocampus at any of the studied time-points (1, 3, 7, 30 dpi). Representative pictures for 1 dpi are shown at Fig. 5. Parvalbumin-, calretinin-, calbindin- and neuropeptide Y- (NPY) positive interneurons were unaffected at all studied time points (data not shown).

NMDA lesion induced progressive neuroinflammation

The infusion of NMDA into the hippocampal formation induced a progressive hypertrophy and activation of microglia (Iba-1 immunoreactivity), which persisted also at 30 dpi of NMDA (Fig. 6). Two-way ANOVA revealed the effect of time (dpi) ($F_{(3, 32)} = 4.156$, $P = 0.0135$), treatment ($F_{(1, 32)} = 51.02$, $P = 0.0001$), as well as their interaction ($F_{(3, 32)} = 6.277$, $P = 0.0018$). Bonferroni's multiple comparison tests showed that the NMDA lesion group differs from the Sham group at 3, 7 and 30 dpi. Infusion of PBS did not induce activation of microglia. Furthermore, the NMDA insult induced significant reactive astrogliosis at all studied time-points (Fig. 7). The astroglial scar persisted even at 30 dpi of NMDA. Two-way ANOVA revealed effect of time ($F_{(3, 32)} = 5.544$, $P = 0.0035$), treatment ($F_{(1, 32)} = 94.41$, $P < 0.0001$), as well as their interaction ($F_{(3, 32)} = 2.944$, $P = 0.0477$). Bonferroni's multiple comparison test showed that NMDA lesion group differs from PBS group at 1, 3, 7 and 30 dpi. Infusion of PBS induced only mild and local astrogliosis at the site of infusion cannula insertion. The increased immunoreactivity for both Iba-1 and GFAP was observed in areas positive for the neurodegeneration marker Fluoro-Jade B (Supplementary Fig. 2).

NMDA lesion induced changes in expression of NMDA and $GABA_A$ receptors subunits

In the next experiment, we investigated the distribution of NMDAR GluN1 and GluN2B subunits in hippocampus. Two-way ANOVA revealed effect of dpi for both subunits (GluN1:

$F_{(3, 31)} = 5.235$, $P = 0.0049$; GluN2B: $F_{(3, 29)} = 4.385$, $P = 0.0116$), treatment (GluN1: $F_{(1, 31)} = 20.81$, $P < 0.0001$; GluN2B: $F_{(1, 29)} = 22.87$, $P < 0.0001$) as well as their interaction (GluN1: $F_{(1, 31)} = 20.81$, $P < 0.0001$; GluN2B: $F_{(1, 31)} = 1.676$, $P = 0.2050$). Bonferroni's multiple comparison test showed that NMDA lesion group differs from sham lesion group at 1 and 3 dpi for both markers. Figures 8 and 9 show the quantification of relative optical density for NMDAR GluN1 and GluN2B subunits, respectively. The increased immunoreactivity correlated positively with FJB positive cells and increased neuroinflammation suggesting that the receptor overexpression is occurring in the lesion affected areas. The changes were reversible and already 7 dpi the NMDA-lesioned animals did not differ from sham group ($P > 0.05$). However, representative pictures suggest that the overexpression of GluN1 as well as GluN2B subunit persisted in lesion-affected areas (Fig. 8 and 9, Supplementary Fig. 2). The contralateral hippocampus was not affected in any group (Supplementary Fig. 3). Furthermore, we analyzed changes in the expression of main $GABA_A$ receptor α1 (Fig. 10), α2 (Fig. 11), α5 (Fig. 12) and γ2 subunits (Fig. 13). NMDA lesion significantly decreased the expression of $GABA_A$ receptor α5 subunit 30 dpi in ipsilateral hippocampus. Two-way ANOVA revealed effect of dpi ($F_{(3, 29)} = 3.243$, $P = 0.0363$), treatment ($F_{(1, 29)} = 5.293$, $P = 0.0288$) as well as their interaction ($F_{(3, 29)} = 2.973$, $P = 0.0480$). Bonferroni's multiple comparison test showed that NMDA lesion group differs from PBS group at 30 dpi. Expression of other subunits was not significantly decreased; however, we observed a mild loss of immunoreactivity in lesion-affected regions. The contralateral hippocampus was not affected in any group (Supplementary Fig. 3).

4. DISCUSSION

Excitotoxins, such as ibotenate, kainate, quisqualate and NMDA have been used to replace traditional tissue ablation techniques (Jarrard, 2002; White et al., 2003; Wallace and Whishaw, 2003; Hoz et al., 2005). Each excitotoxin interacts with specific subgroup of glutamatergic receptors and produces different pattern of damage (Jarrard, 2002). NMDA, the excitotoxin used in this study, interacts specifically with NMDA receptors (Watkins and Evans, 1981). A single unilateral infusion of NMDA into hippocampus induced chronic, focal neurodegeneration around the injection site. The lesion was accompanied by severe and progressive neuroinflammation and affected preferentially principal neurons leaving GABAergic interneurons spared from the damage. We did not observed spread of the damage into the contralateral hippocampus or any other structure. Furthermore, the unilateral lesion did not induced significant impairment of spatial learning abilities. Finally, GluN1 and GluN2B subunits of NMDA receptor were upregulated at 1 and 3 dpi, while $GABA_A$ α5 subunit was downregulated at 30 dpi.

Unilateral infusion of NMDA induced chronic neurodegeneration of hippocampal principal cells

The single unilateral injection of NMDA into hippocampus affected all cell fields of the hippocampus. We did not observe consistently increased FJB staining in any specific subregion of hippocampal formation. Compare to kainate lesion of the hippocampus, NMDA lesion does not produce a uniform and anatomically defined pattern of damage. Single injection of kainate into hippocampus is characterized by loss of hilar neurons, partial loss of CA1 and CA3 and progressive dispersion of dentate gyrus (Bouilleret et al., 2000), whereas NMDA lesion damage pattern was more variable and presumably followed the spread of injected solution. We also did not observe significant hippocampal sclerosis. These data are in accordance with other studies investigating the relationship between the damage pattern and receptor density after administration of different excitotoxins. NMDA was described to induce damage of all hippocampal regions (Jarrard, 2002). However, *ex vivo* experiments in organotypic slices revealed increase vulnerability of CA1, the region of highest NMDA receptor density, followed by granule cells and CA3 after NMDA treatment (Kristensen et al., 2001, Vinet et al., 2012). The discrepancy between *in vivo* and *ex vivo* studies can be explained by the different mode of drug

administration. While the NMDA treatment in *ex vivo* studies allows to apply the drug homogenously on the tissue, the extent of stereotactic infusion is determined by the localization of injection, volume of the infused solution and the tissue diffusion properties.

Interestingly, we found large amounts (25 - 50 %) of FJB positive cells even at 30 dpi. This finding is important for possible interpretations of behavioral studies using this lesion model to "inactivate" hippocampus or any other structure. It seems that NMDA lesion at a mild dose is inducing rather chronic neurodegeneration than a fast ablation of the structure. A high dose of NMDA and multiple infusion sites are required for the successful tissue ablation (White et al., 2003; Wallace and Whishaw, 2003).

The lesion did not spread to other structures and did not induce spatial learning deficit

At the morphological level, the unilateral infusion of NMDA induced focal damage, leaving secondary structures unaffected. We also did not observe conspicuous spread of the damage with MR imaging. In this study, bilateral infusion of NMDA into the hippocampus, but not unilateral, induced significant spatial learning deficit in Carousel maze at 11 dpi. This further supports our finding that the lesion did not affect contralateral hippocampus at morphological level even though they are highly interconnected. It seems that contralateral hippocampus is able to compensate for the lesioned hippocampus performance. Another explanation for this observation might be neural reorganization or partial regeneration of the lesioned hippocampus during the recovery phase. In contrast to our present findings, unilateral inactivation of the hippocampal formation with tetrodoxin, the sodium channel blocker, is known to induce spatial learning deficit in tasks such as Carousel maze (Cimadevilla et al., 2000; Kubik and Fenton, 2005) or Morris water maze (Cimadevilla et al., 2005). However, these reports support the finding that NMDA induced hippocampal damage does not represent a model to inactivate the structure, but rather excitotoxicity triggered neurodegeneration.

NMDA infusion did not affect GABAergic interneurons

Interestingly, we observed that infusion of NMDA did not affect GABAergic interneurons. Neither, immunostaining for parvalbumin-, calbindin-, calretitnin- nor NPY-positive interneurons were affected. In the kainate lesion model in mice, immediate loss of parvalbumin and calbindin positive interneurons in dentate gyrus and CA1 has been described (Bouilleret et

al., 2000). Since we have this model well established in our laboratory, we were able to perform the immunostaining under the same conditions and antibodies also with tissue from kainite-injected animals to have appropriate positive control (data not shown). The loss of calcium-binding proteins is a strong neurodegeneration indicator of interneurons; however, not ultimate evidence. Nevertheless, we did not observe significant changes in expression of $GABA_A$ receptor α1 subunit, which is the marker of majority of interneurons (Gao and Fritschy, 1994). This is, to our knowledge the first report showing a lesser vulnerability of interneurons to NMDA treatment at morphological level. However, another study comparing the sensitivity of CA1 pyramidal neurons with interneurons of stratum oriens reported that interneurons are more resistant and tolerate longer exposure to NMDA (Avignone et al., 2005). Furthermore, they showed that the acute toxicity driving the neurodegeneration of pyramidal cells is independent of intracellular calcium levels and is rather driven by their greater response to the activation of NMDA receptor. It has been also speculated that calcium-binding proteins could buffer Ca^{2+} and thus protect interneurons from its overload. However, knockout experiments (Airaksinen et al., 1997; Schwaller et al., 1999) as well as utilization of Ca^{2+} chelator BAPTA (Avignone et al., 2005) failed to prove this hypothesis. Therefore, we hypothesize that the observed ability of interneurons to resist NMDA excitotoxicity is caused rather by their different responses to NMDA receptor stimulation than the density of expressed NMDA receptors or Ca^{2+} buffering.

Neurodegeneration was accompanied with progressive neuroinflammation

Additionally, we found progressive activation of microglia and reactive astrogliosis in lesion-affected regions. The neuroinflammation persisted even 30 days after the lesion and co-localized with ongoing neurodegeneration (Supplementary Fig. 2). Microglia, the brain resident macrophages, rapidly respond to the neuronal injury by migration to the site of injury (Kreutberg 1996), changing their morphology and expression pattern of its surface markers (Greter et al., 2015), as well as by secretion of a number of signal molecules such as cytokines and chemokines. Importantly, hours after the infusion the blood brain barrier is compromised allowing monocytes as well as lymphocytes to infiltrate brain parenchyma. Iba-1, the microglia marker used in this study, is upregulated during microglia activation; however, it is expressed also in resting microglia. Furthermore, Iba-1 is expressed also on macrophages; hence the observed immunoreactivity may include also invaded monocyte-derived macrophages. Although,

a recent study showed that after kainate lesion the infiltrating myeloid cells ($CD11b^{+}/CD45^{high}$) represent only minor group compare to resident cells (Hong et al., 2010). The activated microglia can have protective as well as negative effects on the ongoing neurodegeneration (Heneka et al., 2014). They are able to remove the damaged neurons and cell debris, protect neurons from damage but also induce further neuroinflammation by secretion of pro-inflammatory cytokines and other factors. A recent study even showed that ramified microglia plays an active protective role against NMDA induced excitotoxicity (Vinet et al., 2012). On the other hand, another study showed that microglia expresses functional NMDA receptors that upon activation may trigger secretion of factors leading to neuronal death (Kaindl et al., 2012). However, we were not able to distinguish their phenotype and role during NMDA induced neurodegeneration with immunohistochemistry. Isolation of microglial cells from the site of injury and consequent analysis of their surface markers would provide better insight into their particular role in this model.

Additionally, we observed a progressive reactive gliosis characterized by increased immunoreactivity of GFAP in lesion-affected regions. It is well known that astrocytes exhibit hypertrophy and proliferate at the site of brain injury (Ridet et al., 1997). Similarly to microglia, astrocytes can influence the lesion outcome in both directions. Formation of a glial scar is changing diffusion parameters and reducing volume of extracellular space (Sykova et al., 1999). This leads to increase of local concentration of neurotransmitters, metabolites as well as reactive oxygen species. The glial scar can also block ongoing regeneration or sprouting of new axons. Although, astrocytes play also an important neuroprotective role. They are capable of scavenging oxygen free radicals and they are buffering extracellular K^{+} and H^{+}, which prevent swelling and glutamate release (Chen and Swanson, 2003).

NMDA infusion induced changes in expression of NMDA and $GABA_A$ receptors subunits

NMDA lesion induced changes in optical density of NMDA and $GABA_A$ receptors subunits immunostaining suggesting changes in their expression. The area of expression changes correlated with ongoing neurodegeneration. We found significantly higher optical density of immunostaining for GluN1 and GluN2B subunits of NMDAR at 1 and 3 dpi. This finding is very surprising considering that the neural tissue should rather protect itself from further excitation. In a transient ischemia model, Liu et al. found significantly increased expression of GluN1 subunit

with at 24h after reperfusion with gradual decrease afterwards (Liu et al., 2010). Another group found increased mRNA levels of GluN1 subunit after kainate injection specifically during status epilepticus (Rafiki et al., 1998). It has been also reported that after pilocarpine-induced status epilepticus, the GluN1 subunit undergoes rapid relocation to the cell surface enhancing excitation in CA3 and DG of rat hippocampus (Naylor et al., 2013). These authors speculate that this rapid upregulation represents a mechanism maintaining status epilepticus and leading to excitotoxic damage. We observed that all animals developed severe seizures lasting hours after the NMDA infusion. The increased expression of NMDA receptor subunits at earlier time points after lesion could therefore be the effect of seizure activity and not direct effect of NMDA.

On the other hand, α5 subunit of $GABA_A$ receptor was significantly downregulated at 30 dpi. $GABA_A$ receptors containing α5 subunit are localized preferentially extrasynaptically at pyramidal cells and generate a tonic conductance that regulates the excitability of pyramidal neurons in CA1 and CA3 regions of the hippocampus (Caraiscos et al., 2004). The loss of α5 subunit immunoreactivity may therefore indicate loss of affected pyramidal cells. Since FJB staining indicates ongoing neurodegeneration by non-specific mechanism (change in intracellular pH), α5 immunohistochemistry might be more specific and sensitive approach to capture temporal progression of neurodegeneration of pyramidal cells. In another work, the immunoreactivity of this subunit was found to be decreased 30 days after kainate lesion in CA1, CA3 and hilus, the regions of cell loss (Bouilleret V. et al., 2000). On the other hand, the loss of α5 subunit on functional neurons may cause disinhibition of pyramidal neurons and shift the inhibitory/excitatory balance towards decreased excitability threshold.

$GABA_A$ α2 subunit is expressed at majority of cells in hippocampus (Fritschy and Mohler, 1995). Semi-quantitative analysis of $GABA_A$ α2 subunit did not show significant loss; however, we observed conspicuous loss at qualitative level in lesion-affected areas only where we found significant downregulation of α5 subunit. This supports the hypothesis that the loss of α5 subunit is connected to loss of pyramidal neuron rather than their downregulation in non affected neurons.

5. CONCLUSIONS

Taken together, our data show that infusion of NMDA into hippocampal formation represents a model of focal, chronic neurodegeneration of principal neurons accompanied by severe neuroinflammation and changes in expression of NMDA receptor GluN1 and GluN2B subunits at an early stage and downregulation of $GABA_A$ receptor α5 subunit at 30 dpi. Surprisingly, GABAergic interneurons seem to be protected from NMDA excitotoxic action. We propose, that this model might be of interest to study chronic neurodegeneration and neuroinflammation, as well as the role of GABAergic interneurons during these processes.

Acknowledgements: This research was supported by following projects: GA UK 604412, SCIEX 11.262, GACR P304/12/G069, P14-20613S, P303/12/1464, „National Institute of Mental Health (NIMH-CZ)“ - grant number ED2.1.00/03.0078 of the ERDF, MH CR-DRO (Institute for Clinical and Experimental Medicine IKEM, IN00023001), OPPK BrainView CZ.2.16/3.1.00/21544 and RVO: 67985823. The authors would like to thank Michaela Fialova for technical assistance.

6. REFERENCES

Airaksinen, M.S., Eilers, J., Garaschuk, O., Thoenen, H., Konnerth, A., Meyer, M., 1997. Ataxia and altered dendritic calcium signaling in mice carrying a targeted null mutation of the calbindin D28k gene. Proc. Natl. Acad. Sci. U. S. A. 94, 1488–93.

Anderson, K.J., Miller, K.M., Fugaccia, I., Scheff, S.W., 2005. Regional distribution of fluoro-jade B staining in the hippocampus following traumatic brain injury. Exp. Neurol. 193, 125–30. doi:10.1016/j.expneurol.2004.11.025

Avignone, E., Frenguelli, B.G., Irving, a J., 2005. Differential responses to NMDA receptor activation in rat hippocampal interneurons and pyramidal cells may underlie enhanced pyramidal cell vulnerability. Eur. J. Neurosci. 22, 3077–90. doi:10.1111/j.1460-9568.2005.04497.x

Bouilleret, V., Loup, F., Kiener, T., Marescaux, C., Fritschy, J.M., 2000. Early loss of interneurons and delayed subunit-specific changes in GABA(A)-receptor expression in a mouse model of mesial temporal lobe epilepsy. Hippocampus 10, 305–324. doi:10.1002/1098-1063(2000)10:3<305::AID-HIPO11>3.0.CO;2-I

Caccamo, D., Campisi, A., Currò, M., Li Volti, G., Vanella, A., Ientile, R., 2004. Excitotoxic and post-ischemic neurodegeneration: Involvement of transglutaminases. Amino Acids. doi:10.1007/s00726-004-0117-1

Caraiscos, V.B., Elliott, E.M., You-Ten, K.E., Cheng, V.Y., Belelli, D., Newell, J.G., Jackson, M.F., Lambert, J.J., Rosahl, T.W., Wafford, K.A., MacDonald, J.F., Orser, B.A., 2004. Tonic inhibition in mouse hippocampal CA1 pyramidal neurons is mediated by alpha5 subunit-containing gamma-aminobutyric acid type A receptors. Proc. Natl. Acad. Sci. U. S. A. 101, 3662–7. doi:10.1073/pnas.0307231101

Chen, Y., Swanson, R.A., 2003. Astrocytes and brain injury. J. Cereb. Blood Flow Metab. 23, 137–49. doi:10.1097/01.WCB.0000044631.80210.3C

Cimadevilla, J.M., Miranda, R., López, L., Arias, J.L., 2005. Partial unilateral inactivation of the dorsal hippocampus impairs spatial memory in the MWM. Cogn. Brain Res. 25, 741–746. doi:10.1016/j.cogbrainres.2005.09.001

Cimadevilla, J.M., Wesierska, M., Fenton, A.A., Bures, J., 2001. Inactivating one hippocampus impairs avoidance of a stable room-defined place during dissociation of arena cues from room cues by rotation of the arena. Proc. Natl. Acad. Sci. U. S. A. 98, 3531–3536. doi:10.1073/pnas.051628398

Cull-Candy, S., Brickley, S., Farrant, M., 2001. NMDA receptor subunits: diversity, development and disease. Curr. Opin. Neurobiol. 11, 327–35.

Dillon, G.M., Qu, X., Marcus, J.N., Dodart, J.-C., 2008. Excitotoxic lesions restricted to the dorsal CA1 field of the hippocampus impair spatial memory and extinction learning in C57BL/6 mice. Neurobiol. Learn. Mem. 90, 426–33. doi:10.1016/j.nlm.2008.05.008

Fenton, A.A., Bures, J., 1993. Place navigation in rats with unilateral tetrodotoxin inactivation of the dorsal hippocampus: place but not procedural learning can be lateralized to one hippocampus. Behav. Neurosci. 107, 552–64.

Fritschy, J.M., Mohler, H., 1995. GABA(A)-receptor heterogeneity in the adult rat brain: Differential regional and cellular distribution of seven major subunits. J. Comp. Neurol. 359, 154–194. doi:10.1002/cne.903590111

Gao, B., Fritschy, J.M., 1994. Selective Allocation of GABA A Receptors Containing the α1 Subunit to Neurochemically Distinct Subpopulations of Rat Hippocampal Interneurons. Eur. J. Neurosci. 6, 837–853. doi:10.1111/j.1460-9568.1994.tb00994.x

Greter, M., Lelios, I., Croxford, A.L., 2015. Microglia Versus Myeloid Cell Nomenclature during Brain Inflammation. Front. Immunol. 6, 249. doi:10.3389/fimmu.2015.00249

Heneka, M.T., Kummer, M.P., Latz, E., 2014. Innate immune activation in neurodegenerative disease. Nat. Rev. Immunol. 14, 463–77. doi:10.1038/nri3705

Hong, J., Cho, I.-H., Kwak, K. Il, Suh, E.C., Seo, J., Min, H.J., Choi, S.-Y., Kim, C.-H., Park, S.H., Jo, E.-K., Lee, S., Lee, K.E., Lee, S.J., 2010. Microglial Toll-like receptor 2 contributes to kainic acid-induced glial activation and hippocampal neuronal cell death. J. Biol. Chem. 285, 39447–57. doi:10.1074/jbc.M110.132522

Jarrard, L.E., 2002. Use of excitotoxins to lesion the hippocampus: Update. Hippocampus 12, 405–414. doi:10.1002/hipo.10054

Kaindl, A.M., Degos, V., Peineau, S., Gouadon, E., Chhor, V., Loron, G., Le Charpentier, T., Josserand, J., Ali, C., Vivien, D., Collingridge, G.L., Lombet, A., Issa, L., Rene, F., Loeffler, J.-P., Kavelaars, A., Verney, C., Mantz, J., Gressens, P., 2012. Activation of microglial N-methyl-D-aspartate receptors triggers inflammation and neuronal cell death in the developing and mature brain. Ann. Neurol. 72, 536–49. doi:10.1002/ana.23626

Kim, S.M., Frank, L.M., 2009. Hippocampal lesions impair rapid learning of a continuous spatial alternation task. PLoS One 4. doi:10.1371/journal.pone.0005494

Kreutzberg, G.W., 1996. Microglia: a sensor for pathological events in the CNS. Trends Neurosci. 19, 312–8.

Kristensen, B.W., Noraberg, J., Zimmer, J., 2001. Comparison of excitotoxic profiles of ATPA, AMPA, KA and NMDA in organotypic hippocampal slice cultures. Brain Res. 917, 21–44. doi:10.1016/S0006-8993(01)02900-6

Kubik, S., Fenton, A.A., 2005. Behavioral evidence that segregation and representation are dissociable hippocampal functions. J. Neurosci. 25, 9205–12. doi:10.1523/JNEUROSCI.1707-05.2005

Lai, T.W., Zhang, S., Wang, Y.T., 2014. Excitotoxicity and stroke: identifying novel targets for neuroprotection. Prog. Neurobiol. 115, 157–88. doi:10.1016/j.pneurobio.2013.11.006

Li, H., Matsumoto, K., Watanabe, H., 1999. Different effects of unilateral and bilateral hippocampal lesions in rats on the performance of radial maze and odor-paired associate tasks. Brain Res. Bull. 48, 113–119. doi:10.1016/S0361-9230(98)00157-9

Li, L., Lundkvist, A., Andersson, D., Wilhelmsson, U., Nagai, N., Pardo, A.C., Nodin, C., Ståhlberg, A., Aprico, K., Larsson, K., Yabe, T., Moons, L., Fotheringham, A., Davies, I., Carmeliet, P., Schwartz, J.P., Pekna, M., Kubista, M., Blomstrand, F., Maragakis, N., Nilsson, M., Pekny, M., 2008. Protective role of reactive astrocytes in brain ischemia. J. Cereb. Blood Flow Metab. 28, 468–481. doi:10.1038/sj.jcbfm.9600546

Liu, Z., Zhao, W., Xu, T., Pei, D., Peng, Y., 2010. Alterations of NMDA receptor subunits NR1, NR2A and NR2B mRNA expression and their relationship to apoptosis following transient forebrain ischemia. Brain Res. 1361, 133–9. doi:10.1016/j.brainres.2010.09.035

Maren, S., 1999. Neurotoxic basolateral amygdala lesions impair learning and memory but not the performance of conditional fear in rats. J. Neurosci. 19, 8696–703.

Maren, S., Aharonov, G., Fanselow, M.S., 1997. Neurotoxic lesions of the dorsal hippocampus and Pavlovian fear conditioning in rats. Behav. Brain Res. 88, 261–274. doi:10.1016/S0166-4328(97)00088-0

Mares, P., Velisek, L., 1992. N-methyl-D-aspartate (NMDA)-induced seizures in developing rats. Dev. Brain Res. 65, 185–189. doi:10.1016/0165-3806(92)90178-Y

Mehta, A., Prabhakar, M., Kumar, P., Deshmukh, R., Sharma, P.L., 2013. Excitotoxicity: Bridge to various triggers in neurodegenerative disorders. Eur. J. Pharmacol. doi:10.1016/j.ejphar.2012.10.032

Naylor, D.E., Liu, H., Niquet, J., Wasterlain, C.G., 2013. Rapid surface accumulation of NMDA receptors increases glutamatergic excitation during status epilepticus. Neurobiol. Dis. 54, 225–238. doi:10.1016/j.nbd.2012.12.015

Paoletti, P., Neyton, J., 2007. NMDA receptor subunits: function and pharmacology. Curr. Opin. Pharmacol. 7, 39–47. doi:10.1016/j.coph.2006.08.011

Paxinos, G., Watson, C., 1998. The Rat Brain in Stereotaxic Coordinates. Elsevier Academic Press.

Rafiki, a, Ben-Ari, Y., Khrestchatisky, M., Represa, a, 1998. Long-lasting enhanced expression in the rat hippocampus of NMDAR1 splice variants in a kainate model of epilepsy [In Process Citation]. Eur J Neurosci 10, 497–507.

Rambousek, L., Bubenikova-Valesova, V., Kacer, P., Syslova, K., Kenney, J., Holubova, K., Najmanova, V., Zach, P., Svoboda, J., Stuchlik, A., Chodounska, H., Kapras, V., Adamusova, E., Borovska, J., Vyklicky, L., Vales, K., 2011. Cellular and behavioural effects of a new steroidal inhibitor of the N-methyl-D-aspartate receptor 3α5β-pregnanolone glutamate. Neuropharmacology 61, 61–68. doi:10.1016/j.neuropharm.2011.02.018

Ridet, J.L., Malhotra, S.K., Privat, A., Gage, F.H., 1997. Reactive astrocytes: cellular and molecular cues to biological function. Trends Neurosci. 20, 570–7.

Sattler, R., Tymianski, M., 2001. Molecular mechanisms of glutamate receptor-mediated excitotoxic neuronal cell death. Mol. Neurobiol. 24, 107–129. doi:10.1385/MN:24:1-3:107

Schmued, L.C., Hopkins, K.J., 2000. Fluoro-Jade B: a high affinity fluorescent marker for the localization of neuronal degeneration. Brain Res. 874, 123–30.

Schwaller, B., Dick, J., Dhoot, G., Carroll, S., Vrbova, G., Nicotera, P., Pette, D., Wyss, A., Bluethmann, H., Hunziker, W., Celio, M.R., 1999. Prolonged contraction-relaxation cycle of fast-twitch muscles in parvalbumin knockout mice. Am. J. Physiol. 276, C395–403.

Sheng, M., Kim, M.J., 2002. Postsynaptic signaling and plasticity mechanisms. Science 298, 776–80. doi:10.1126/science.1075333

Sparks, F.T., Lehmann, H., Hernandez, K., Sutherland, R.J., 2011. Suppression of neurotoxic lesion-induced seizure activity: evidence for a permanent role for the hippocampus in contextual memory. PLoS One 6, e27426. doi:10.1371/journal.pone.0027426

Stuchlik, A., Kubik, S., Vlcek, K., Vales, K., 2014. Spatial navigation: implications for animal models, drug development and human studies. Physiol. Res. 63 Suppl 1, S237–49.

Stuchlik, A., Petrasek, T., Prokopova, I., Holubova, K., Hatalova, H., Vales, K., Kubik, S., Dockery, C., Wesierska, M., 2013. Place avoidance tasks as tools in the behavioral neuroscience of learning and memory. Physiol. Res.

Stuchlik, A., Rezacova, L., Vales, K., Bubenikova, V., Kubik, S., 2004. Application of a novel Active Allothetic Place Avoidance task (AAPA) in testing a pharmacological model of psychosis in rats: Comparison with the Morris Water Maze. Neurosci. Lett. 366, 162–166. doi:10.1016/j.neulet.2004.05.037

Sykova, E., Roitbak, T., Mazel, T., Simonova, Z., Harvey, A.R., 1999. Astrocytes, oligodendroglia, extracellular space volume and geometry in rat fetal brain grafts. Neuroscience 91, 783–798. doi:10.1016/S0306-4522(98)00603-4

Vinet, J., van Weering, H.R., Heinrich, A., Kälin, R.E., Wegner, A., Brouwer, N., Heppner, F.L., van Rooijen, N., Boddeke, H.W., Biber, K., 2012. Neuroprotective function for ramified microglia in hippocampal excitotoxicity. J. Neuroinflammation 9, 27. doi:10.1186/1742-2094-9-27

Wallace, D.G., Whishaw, I.Q., 2003. NMDA lesions of Ammon's horn and the dentate gyrus disrupt the direct and temporally paced homing displayed by rats exploring a novel environment: Evidence for a role of the hippocampus in dead reckoning. Eur. J. Neurosci. 18, 513–523. doi:10.1046/j.1460-9568.2003.02772.x

Watanabe, M., Fukaya, M., Sakimura, K., Manabe, T., Mishina, M., Inoue, Y., 1998. Selective scarcity of NMDA receptor channel subunits in the stratum lucidum (mossy fibre-recipient layer) of the mouse hippocampal CA3 subfield. Eur. J. Neurosci. 10, 478–487. doi:10.1046/j.1460-9568.1998.00063.x

Watkins, J.C., Evans, R.H., 1981. Excitatory Amino Acid Transmitters. Annu. Rev. Pharmacol. Toxicol. 21, 165–204. doi:10.1146/annurev.pa.21.040181.001121

White, N.M., Holahan, M.R., Goffaux, P., 2003. Involuntary, unreinforced (pure) spatial learning is impaired by fimbria-fornix but not by dorsal hippocampus lesions. Hippocampus 13, 324–333. doi:10.1002/hipo.10080

Zaczek, R., Coyle, J.T., 1982. Excitatory amino acid analogues: Neurotoxicity and seizures. Neuropharmacology 21, 15–26. doi:10.1016/0028-3908(82)90205-2

Zukin, R.S., Bennett, M. V, 1995. Alternatively spliced isoforms of the NMDARI receptor subunit. Trends Neurosci. 18, 306–13.

TABLE AND FIGURE LEGENDS

Table 1: List of primary antibodies, their manufacturers and dilutions used.

Figure 1: Representative images of Fluoro-Jade B staining of dorsal ipsilateral hippocampus at 1, 3, 7 and 30 dpi after the infusion of NMDA or PBS (1 dpi). Scale bar: A = 500 μm.

Figure 2: Volumetric analysis of ipsilateral hippocampus did not reveal significant changes over 30 days after NMDA infusion ($P > 0.05$). Values are given as mean ± SEM, (n = 5).

Figure 3: Representative axial (left panel) and coronal (right panel) T_2 weighted images of rat brain before and after infusion of NMDA into hippocampus. Figures illustrate the track of infusion cannula as well the extent of lesion up to 7 dpi. Infusion of NMDA increased the T_2 signal suggesting edema and inflammation in ipsilateral hippocampus.

Figure 4: Unilateral (uni) infusion of NMDA (25 and 50 mM) did not induce spatial learning deficit measured as number of entrances into forbidden sector in the Carousel Maze. On the other hand, bilateral (bi) infusion induced significant spatial learning deficit (* $p < 0.05$, ** $p < 0.01$). Rats were tested 7 days after surgery in four consecutive sessions. The represented data are thus from day 11 after NMDA infusion. Values are given as mean ± SEM.

Figure 5: Distribution of parvalbumin, neuropeptide Y, calbindin and calretinin immunoreactivity 1 day after PBS or NMDA injection into hippocampus. Scale bar = 500 μm.

Figure 6: Representative images of immunoperoxidase staining using anti-Iba-1 antibody taken from the ipsilateral dorsal hippocampus at 1, 3, 7 or 30 dpi of NMDA or PBS (1 dpi). Scale bar: A = 500 μm. The chart in right bottom corner shows quantitative analysis of hippocampal anti-Iba-1 immunoreactivity (IR) representing relative percentage of area covered by activated microglia. Values are given as mean ± SEM. ** $P < 0.01$, *** $P < 0.001$.

Figure 7: Representative images of immunoperoxidase staining using anti-GFAP antibody taken from the ipsilateral dorsal hippocampus at 1, 3, 7 or 30 dpi of NMDA or PBS. Scale bar: A = 500 μm. The chart in right bottom corner shows quantitative analysis of hippocampal anti-GFAP immunoreactivity (IR) representing relative percentage of area covered by astrocytes. Values are given as mean ± SEM. * $P < 0.05$, *** $P < 0.001$.

Figure 8: Representative images of immunoperoxidase staining using anti-NMDA receptor GluN1 subunit antibody taken from the ipsilateral dorsal hippocampus at 1, 3, 7 or 30 dpi of NMDA or PBS (1 dpi). We did not observe significant changes in PBS injected hippocampus. NMDA lesion induced significant overexpression of NMDA receptor NR1 subunit in ipsilateral hippocampus at 1 and 3 dpi ($P < 0.05$). Scale bar: A = 500 μm. The chart in right bottom corner shows quantitative analysis of immunoperoxidase staining relative optical density. Values are given as mean ± SEM. * $P < 0.05$, ** $P < 0.005$.

Figure 9: Representative images of immunoperoxidase staining using anti-NMDA receptor GluN2B subunit antibody taken from the ipsilateral dorsal hippocampus at 1, 3, 7 or 30 dpi of NMDA or PBS (1 dpi). We did not observe significant changes in PBS injected hippocampus. NMDA lesion induced overexpression of NMDA receptor NR2B subunit in ipsilateral hippocampus ($P < 0.05$). The overexpression was significant at 1 and 3. The overexpression correlated with activation of microglia. Scale bar: A = 500 μm. The chart in right bottom corner shows quantitative analysis of immunoperoxidase staining relative optical density. Values are given as mean ± SEM. * $P < 0.05$, ** $P < 0.005$.

Figure 10: Representative images of immunoperoxidase staining using anti-$GABA_A$ receptor α_1 subunit antibody taken from the ipsilateral dorsal hippocampus at 1, 3, 7 or 30 dpi of NMDA or PBS (1 dpi). We did not observe significant changes in PBS injected hippocampus. NMDA did not induce significant changes in α_1 subunit expression ($P > 0.05$). We also did not observed loss of $GABA_A$ receptor α_1 interneurons at any time-point. Scale bar: A = 500 μm. The chart in right bottom corner shows quantitative analysis of immunoperoxidase staining relative optical density. Values are given as mean ± SEM.

Figure 11: Representative images of immunoperoxidase staining using anti-$GABA_A$ receptor α2 subunit antibody taken from the ipsilateral dorsal hippocampus at 1, 3, 7 or 30 dpi of NMDA or PBS (1 dpi). We did not observe significant changes in PBS injected hippocampus. Quantification of relative optical density did not reveal significant changes between NMDA and PBS injected hippocampus ($P > 0.05$); however, we observed local loss of α2 subunit staining at days 7 and 30dpi that correlated with activation of microglia. Scale bar: A = 500 μm. The chart in right bottom corner shows quantitative analysis of immunoperoxidase staining relative optical density. Values are given as mean ± SEM.

Figure 12: Representative images of immunoperoxidase staining using anti-$GABA_A$ receptor α5 subunit antibody taken from the ipsilateral dorsal hippocampus at 1, 3, 7 or 30 dpi of NMDA or PBS (1 dpi). We did not observe significant changes in PBS injected hippocampus. NMDA induced progressive loss of α5 subunit expression. The expression was significantly different compare to PBS sham lesion at 30 dpi ($P < 0.05$). Scale bar: A = 500 μm. The chart in right bottom corner shows quantitative analysis of immunoperoxidase staining relative optical density. Values are given as mean ± SEM. * $P < 0.05$.

Figure 13: Representative images of immunoperoxidase staining using anti-$GABA_A$ receptor γ2 subunit antibody taken from the ipsilateral dorsal hippocampus at 1, 3, 7 or 30 dpi of NMDA or PBS (1 dpi). We did not observe significant changes in PBS injected hippocampus. Quantification of relative optical density did not reveal significant changes between NMDA and PBS injected hippocampus ($P > 0.05$). Scale bar: A = 500 μm. The chart in right bottom corner

shows quantitative analysis of immunoperoxidase staining relative optical density. Values are given as mean ± SEM.

Supplementary Figure 1: Neural damage score after the NMDA lesion of hippocampus at 1, 3, 7 and 30 dpi in CA1, CA3, dentate gyrus (DG), hilus and subiculum. No significant differences were observed among individual dpi. Sham lesion induced no damage (score 0, data not shown) Score scale: 0 – 0-5%, 1 – 6-25%, 2 – 26-50%, 3 – 51-75%, 4 > 75%.

Supplementary Figure 2: Representative picture of dorsal hippocampus from the same animal demonstrating colocalization of the changes induced by unilateral infusion of NMDA at 30 dpi. Fluoro-Jade B, A = 500 μm; DAB stainings B = 500 μm.

Supplementary Figure 3: Quantitative analysis of immunoperoxidase staining relative optical density in contralateral (intact) hippocampus. Statistical analysis did not reveal any difference between NMDA and PBS group ($P > 0.05$). Values are given as mean ± SEM.

Antibody	**Manufacturer**	**Description/Nr.**	**Dilution**
$GABA_AR$ α1	Fritschy and Möhler, 1995	Home-made guinea pig antiserum	1:20000
$GABA_AR$ α2	Fritschy and Möhler, 1995	Home-made affinity-purified guinea pig antiserum	1:1000
$GABA_AR$ α5	Fritschy and Möhler, 1995	Home-made Guinea pig antiserum	1:3000
$GABA_AR$ γ2	Fritschy and Möhler, 1995	Home-made Guinea pig antiserum	1:15000
NMDAR GluN1	NeuroMab, CA, USA	Mouse monoclonal, clone N308/48	1:2000
NMDAR GluN2B	NeuroMab,CA, USA	Mouse monoclonal, clone N59/36	1:2000
Iba-1	Wako	Rabbit polyclonal, 019-19741	1:4000
GFAP	Dako Schweiz AG, Switzerland	Rabbit polyclonal, Z334	1:5000
Parvalbumin	SWant, Switzerland	Rabbit polyclonal, PV-25	1:5000
Calretinin	SWant, Switzerland	Rabbit serum, 7696	1:2000
Calbindin	SWant, Switzerland	Rabbit serum, CB-38	1:3000
NPY	Peninsula Laboratories, USA	Rabbit serum, T4069	1:1000

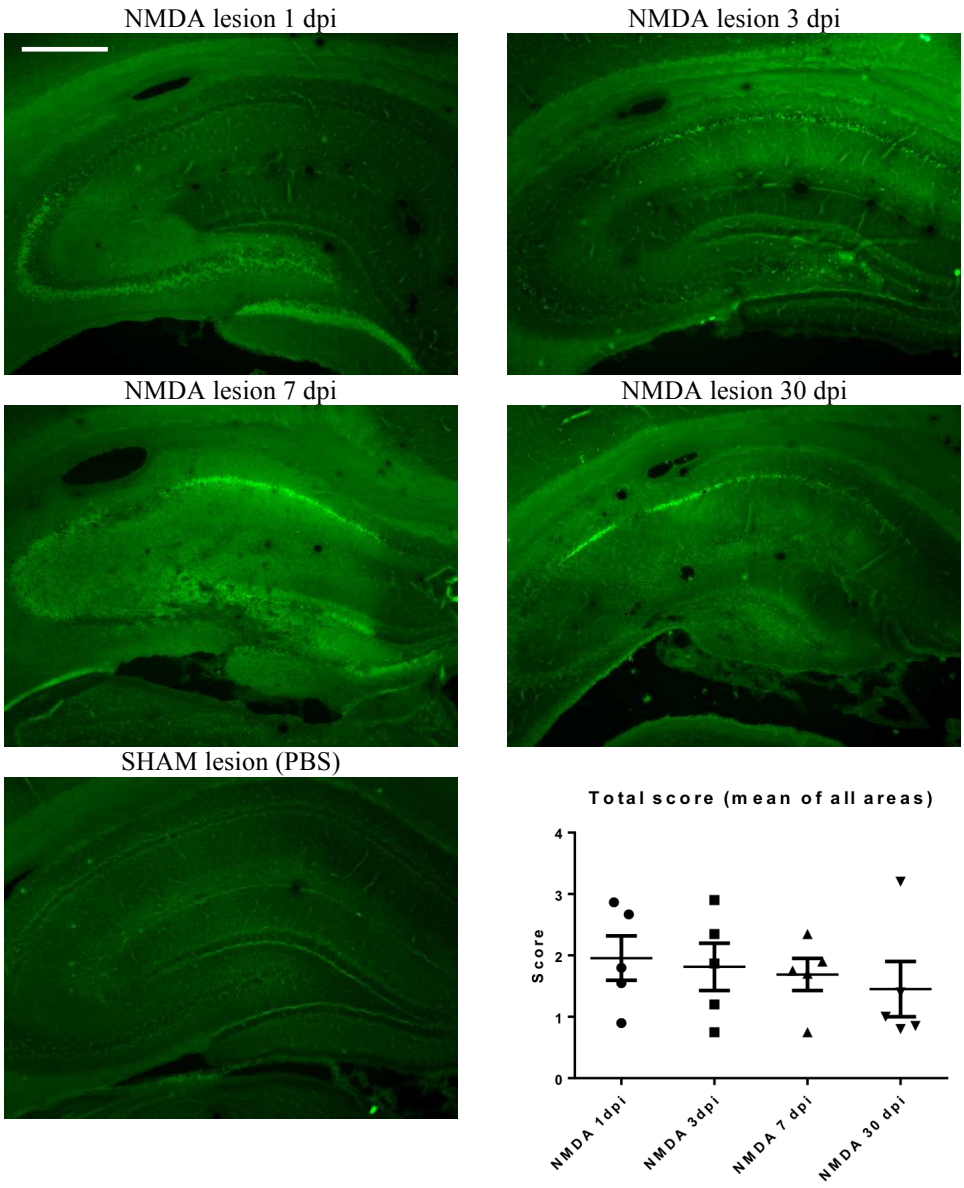

Figure 1A: Representative images of Fluoro-Jade B staining of dorsal ipsilateral hippocampus at 1, 3, 7 or 30 dpi of NMDA or PBS (1 dpi). Scale bar: A = 500 µm.

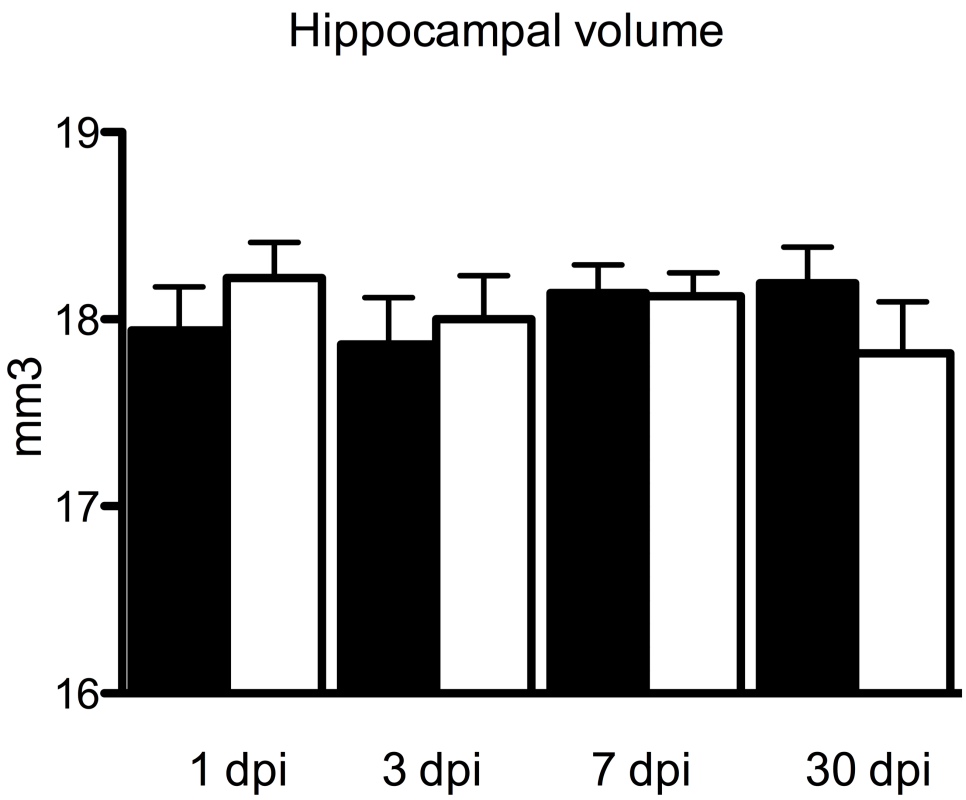

Figure 1B: Volumetric analysis of ipsilateral hippocampus did not reveal significant changes over 30 days after NMDA infusion ($P > 0.05$). Values are given as mean ± SEM, ($n = 5$).

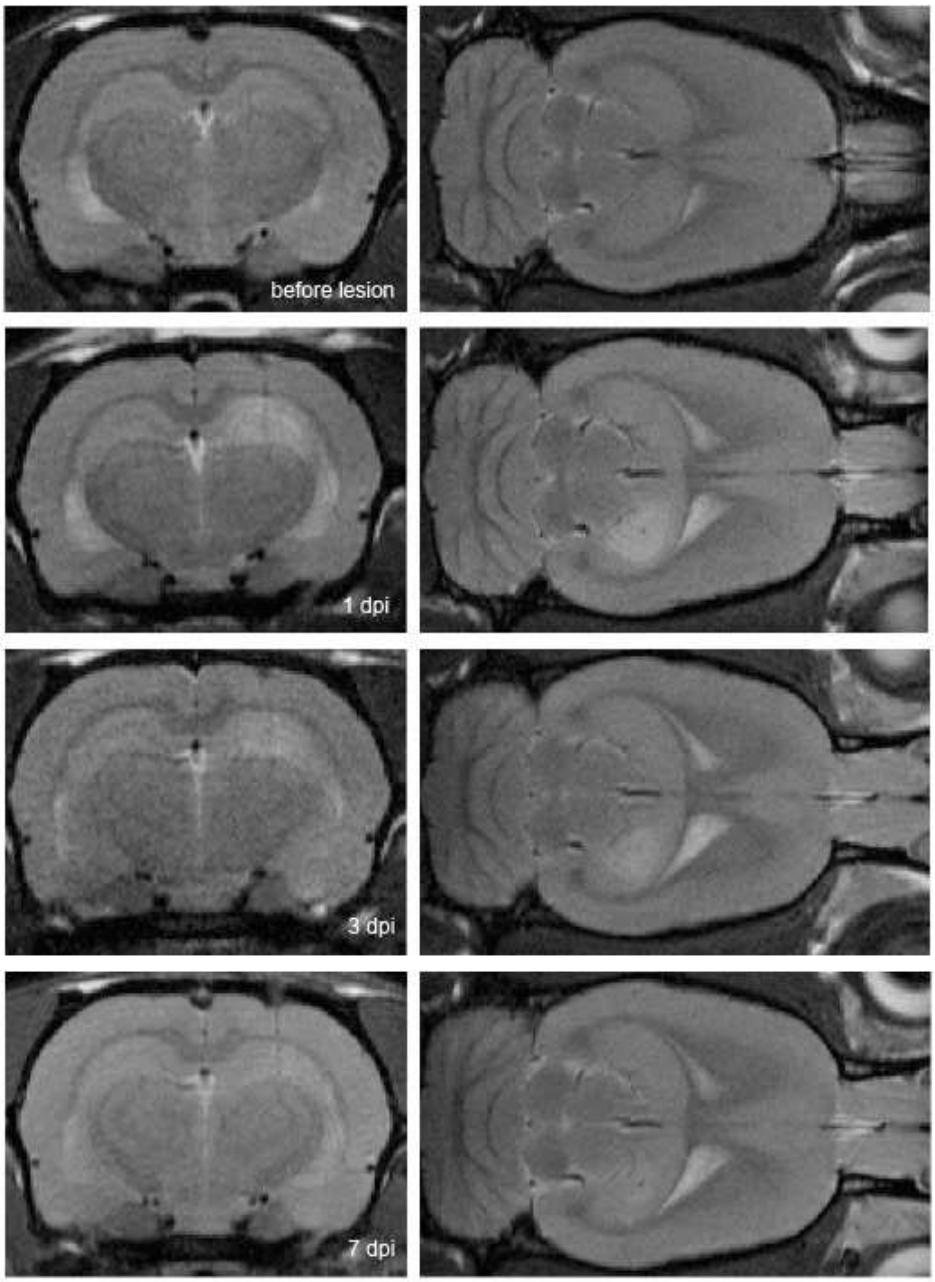

Figure 2: Representative coronal (left panel) and sagittal (right panel) T2 weighted images of rat brain before and after infusion of NMDA into hippocampus. Pictures illustrate the track of infusion cannula as well the extent of lesion up to 7 days post injection (dpi). Infusion of NMDA increased the T2 signal suggesting edema and inflammation in ipsilateral hippocampus.

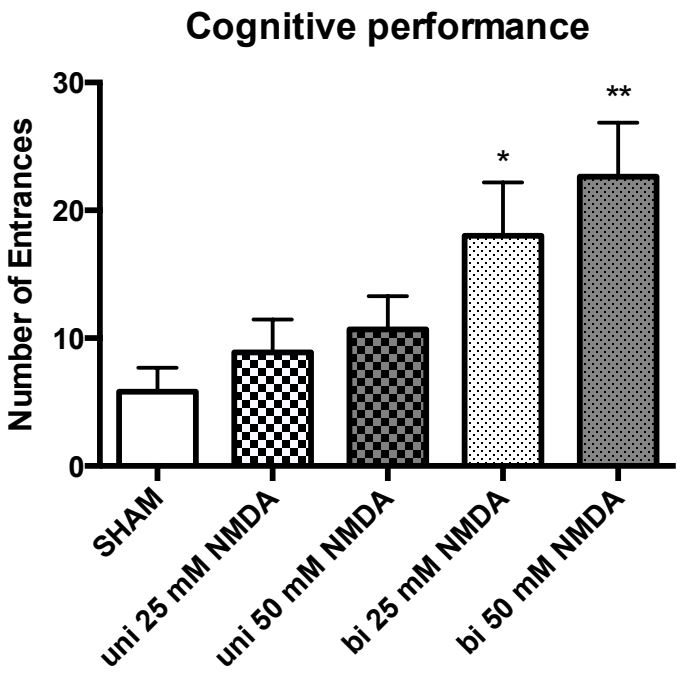

Figure 3: Unilateral infusion of NMDA (25 and 50 mM) did not induce spatial learning deficit measured as number of entrances into forbidden sector in Carousel Maze. On the other hand, bilateral infusion induced significant spatial learning deficit (* $p < 0.05$, ** $p < 0.01$). Rats were tested 7 days after surgery in four consecutive sessions. The represented data are thus from day 11 after NMDA infusion. Values are given as mean ± SEM.

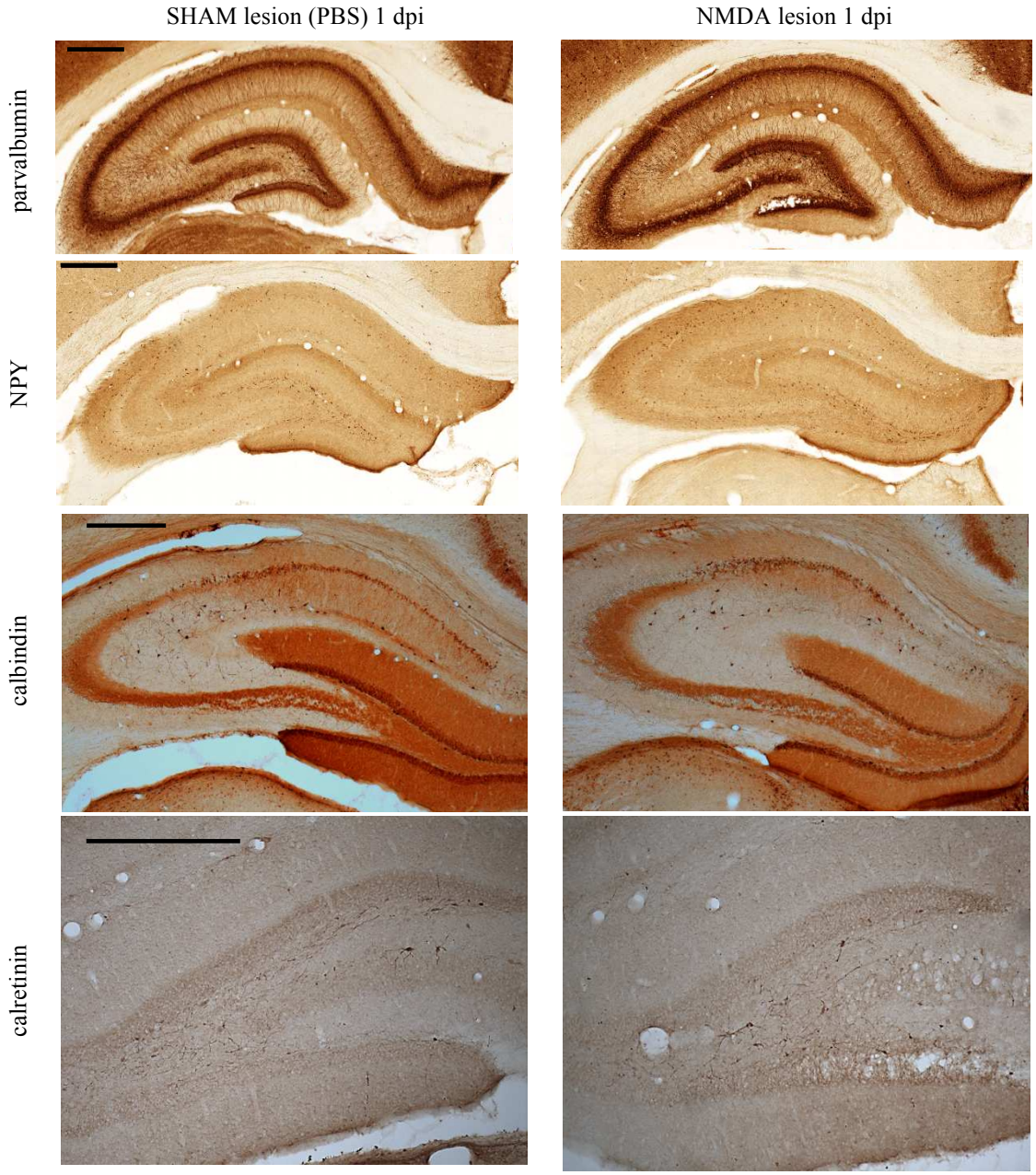

Figure 4: Distribution of parvalbumin, neuropeptide Y (NPY), calbindin and calretinin immunoreactivity 1 day after PBS or NMDA injection into hippocampus. Scale bar: A = 500 µm.

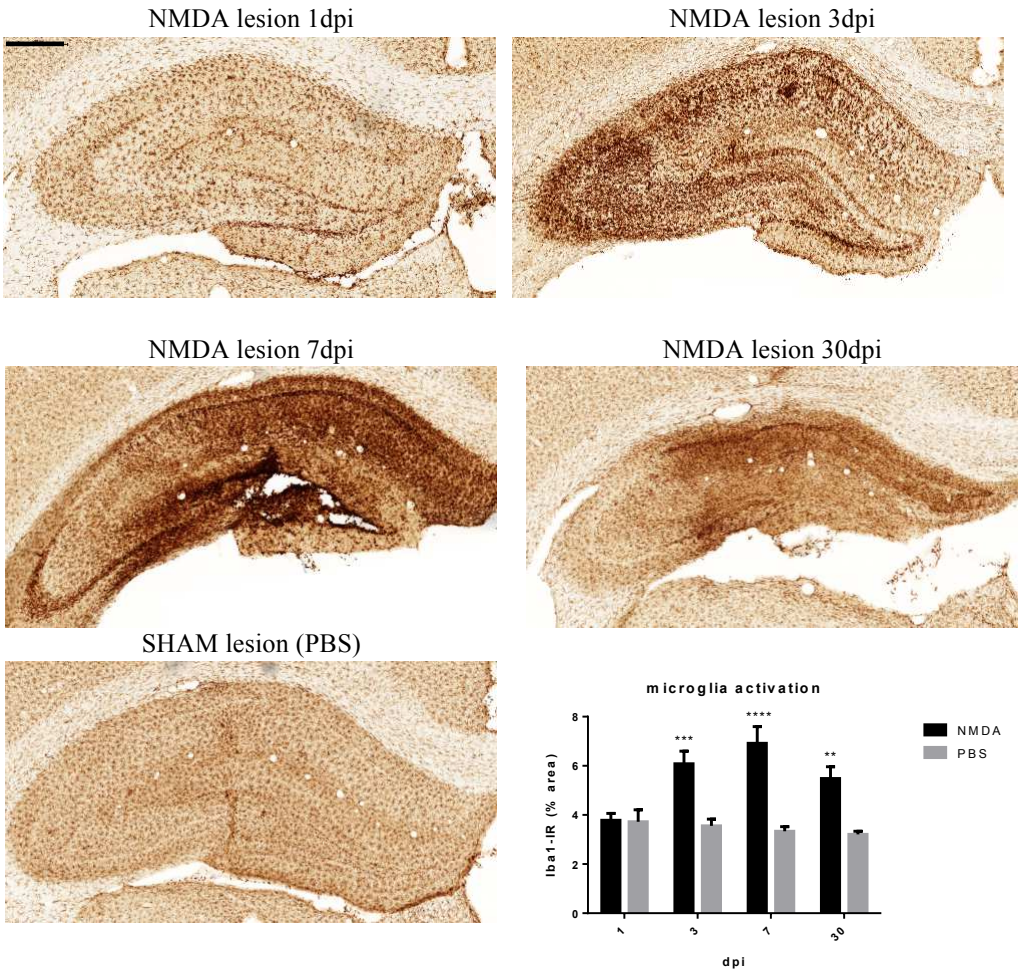

Figure 5: A: Representative images of immunoperoxidase staining using anti-Iba-1 antibody taken from the ipsilateral dorsal hippocampus at 1, 3, 7 or 30 days post injection (dpi) of NMDA or PBS. Scale bar: A = 500 µm. B: Quantitative analysis of hippocampal anti-Iba-1 immunoreactivity (IR) representing relative percentage of area covered by activated microglia. Values are given as mean ± SEM. ** $P < 0.01$, *** $P < 0.001$, **** $P < 0.0001$.

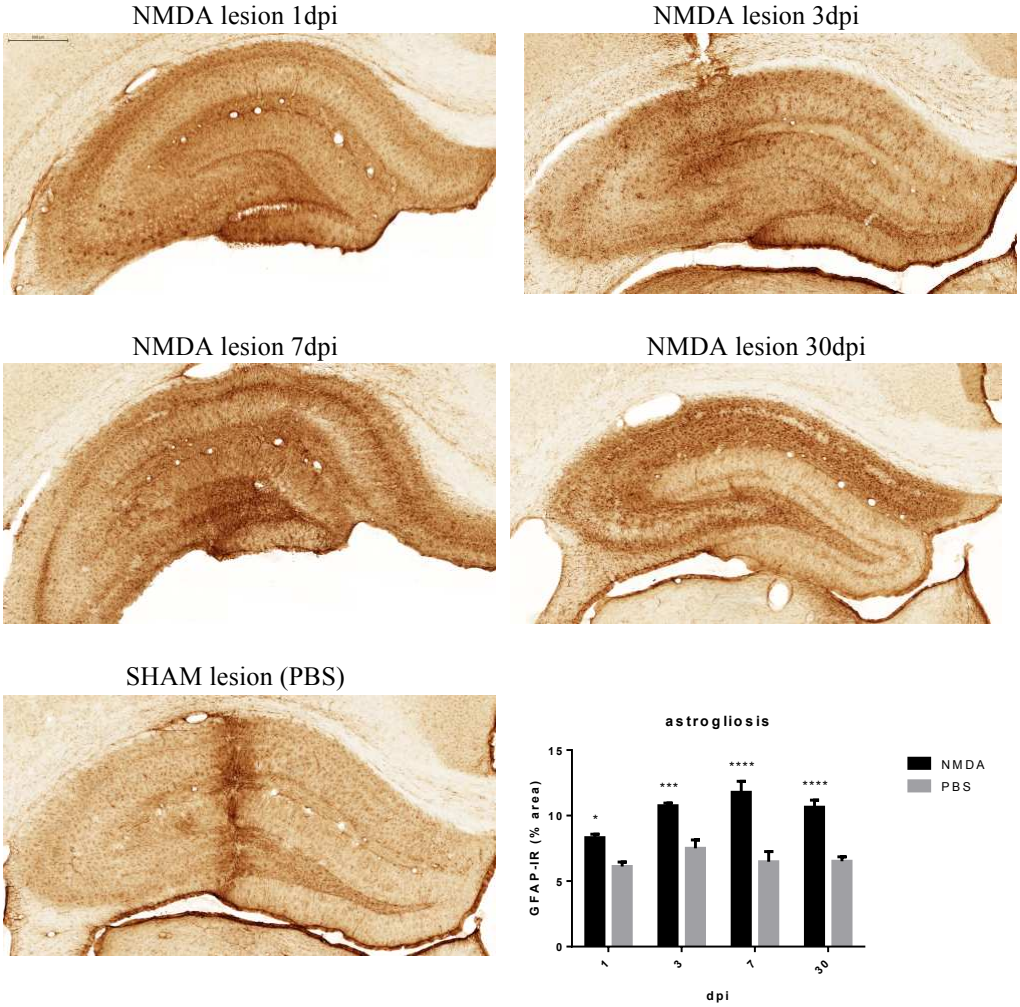

Figure 6: A: Representative images of immunoperoxidase staining using anti-GFAP antibody taken from the ipsilateral dorsal hippocampus at 1, 3, 7 or 30 days post injection (dpi) of NMDA or PBS. Scale bar: A = 500 µm. B: Quantitative analysis of hippocampal anti-GFAP immunoreactivity (IR) representing relative percentage of area covered by astrocytes. Values are given as mean ± SEM. * $P < 0.05$, *** $P < 0.001$, **** $P < 0.0001$.

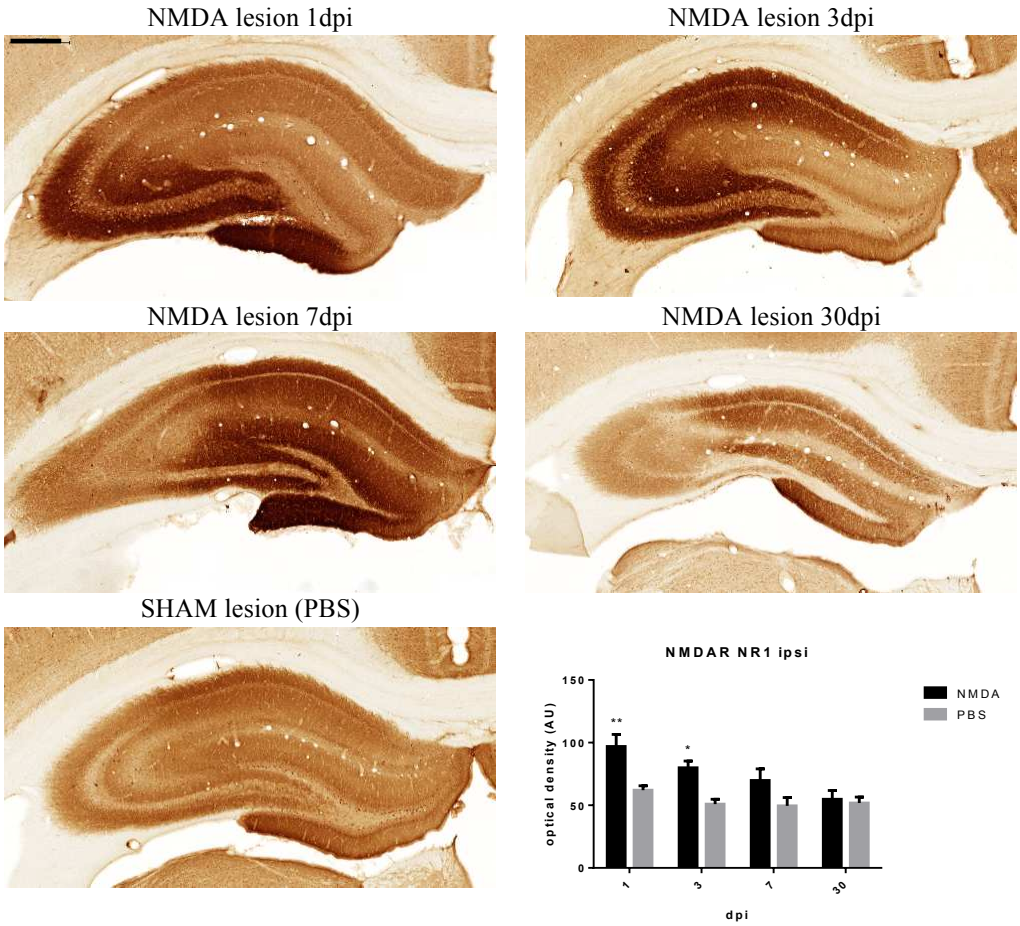

Figure 7: A: Representative images of immunoperoxidase staining using anti-NMDA receptor NR1 subunit antibody taken from the ipsilateral dorsal hippocampus at 1, 3, 7 or 30 days post injection (dpi) of NMDA. We did not observe significant changes in PBS injected hippocampus. NMDA lesion induced significant overexpression of NMDA receptor NR1 subunit in ipsilateral hippocampus at 1 a 3 days post injection (dpi) of NMDA ($P < 0.05$). Scale bar: A = 500 µm. B: Quantitative analysis of immunoperoxidase staining relative optical density. Values are given as mean ± SEM. * $P < 0.05$, ** $P < 0.005$.

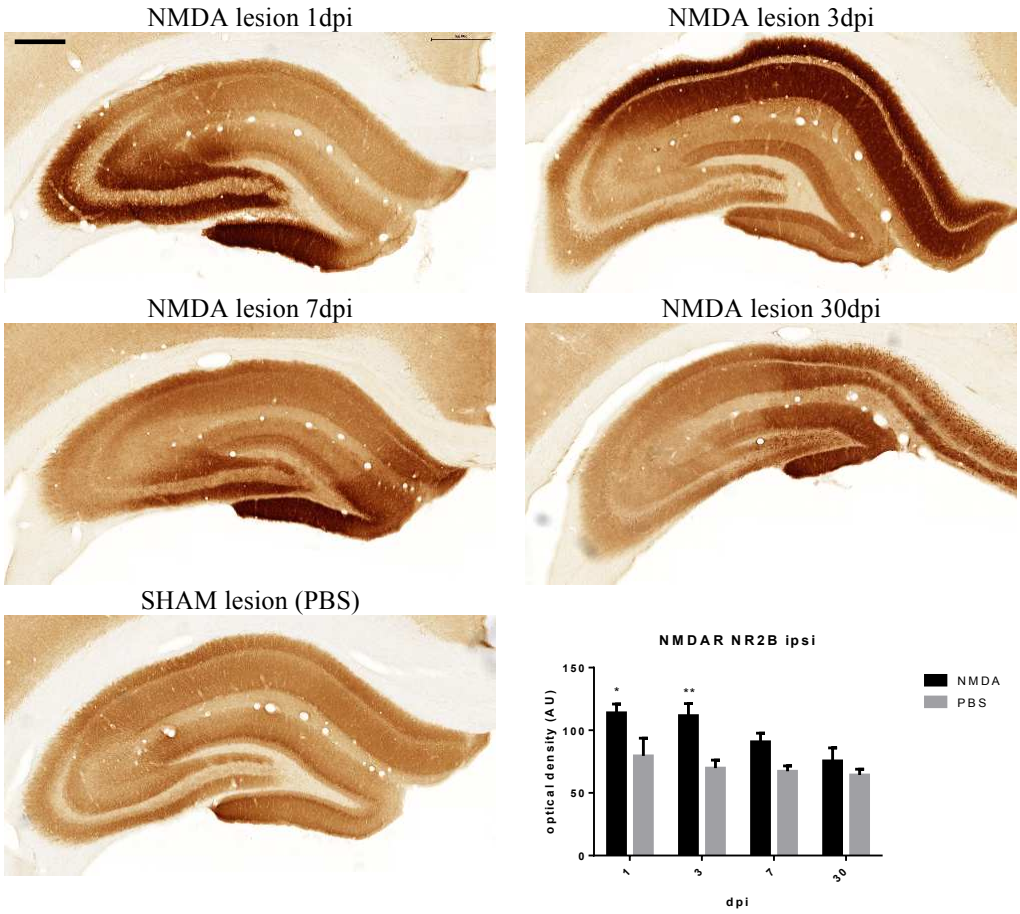

Figure 8: A: Representative images of immunoperoxidase staining using anti-NMDA receptor NR2B subunit antibody taken from the ipsilateral dorsal hippocampus at 1, 3, 7 or 30 days post injection (dpi) of NMDA. We did not observe significant changes in PBS injected hippocampus; therefore only one representative picture is shown. NMDA lesion induced overexpression of NMDA receptor NR2B subunit in ipsilateral hippocampus ($P < 0.05$). The overexpression was significant 1 a 3 days post injection (dpi) of NMDA. The overexpression correlated with activation of microglia. Scale bar: A = 500 µm. B: Quantitative analysis of immunoperoxidase staining relative optical density. Values are given as mean ± SEM. * $P < 0.05$, ** $P < 0.005$.

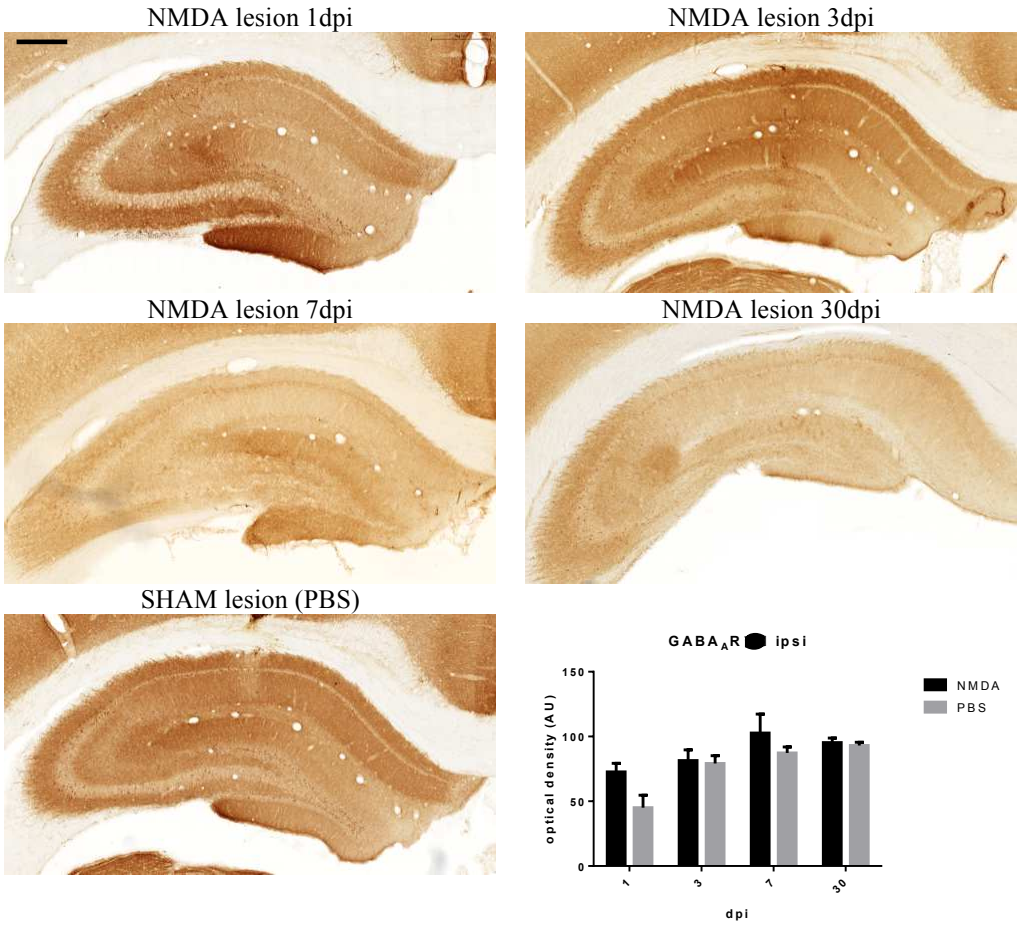

Figure 9: A: Representative images of immunoperoxidase staining using anti-$GABA_A$ receptor α_1 subunit antibody taken from the ipsilateral dorsal hippocampus at 1, 3, 7 or 30 days post injection (dpi) of NMDA. We did not observe significant changes in PBS injected hippocampus. NMDA did not induce significant changes in α_1 subunit expression ($P > 0.05$). We also did not observed loss of $GABA_A$ receptor α_1 interneurons at any time-point. Scale bar: A = 500 µm. B: Quantitative analysis of immunoperoxidase staining relative optical density. Values are given as mean ± SEM.

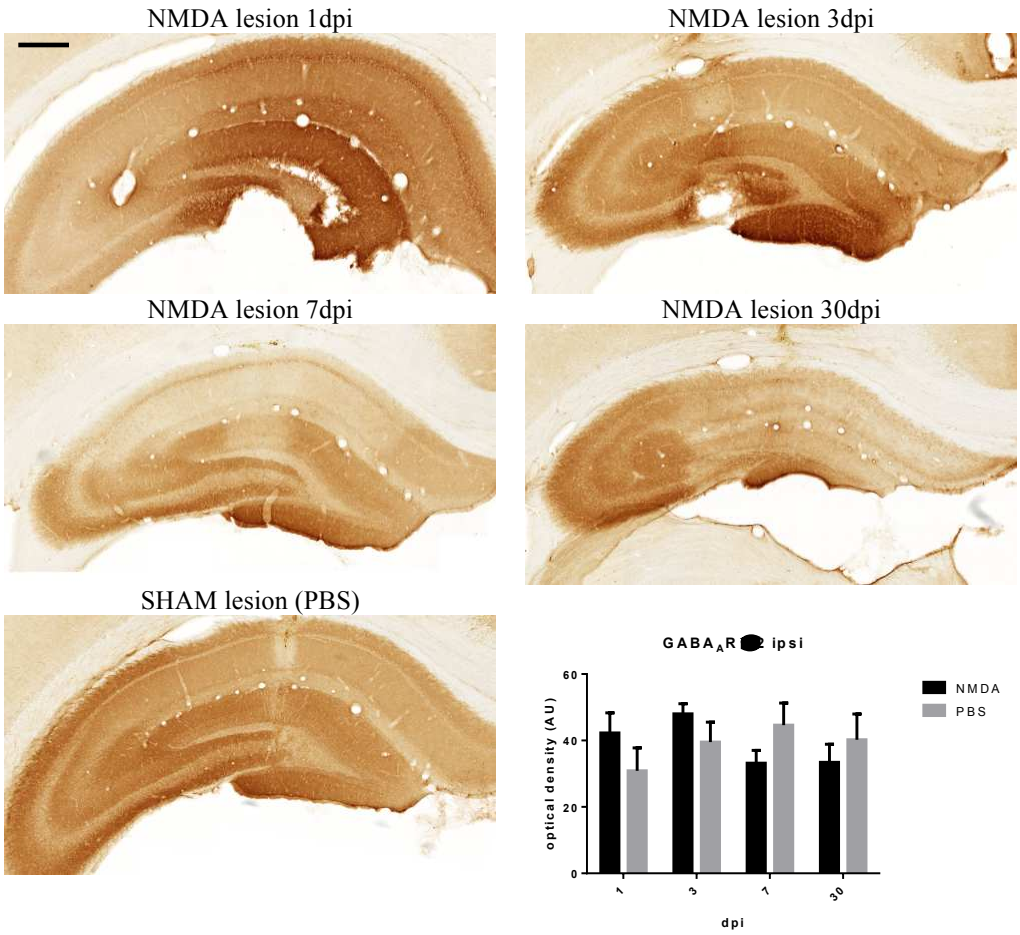

Figure 10: A: Representative images of immunoperoxidase staining using anti-$GABA_A$ receptor α2 subunit antibody taken from the ipsilateral dorsal hippocampus at 1, 3, 7 or 30 days post injection (dpi) of NMDA. We did not observe significant changes in PBS injected hippocampus. Quantification of relative optical density did not reveal significant changes between NMDA and PBS injected hippocampus ($P > 0.05$); however, we observed local loss of α2 subunit staining at days 7 and 30dpi that correlated with activation of microglia. Scale bar: A = 500 µm. B: Quantitative analysis of immunoperoxidase staining relative optical density. Values are given as mean ± SEM.

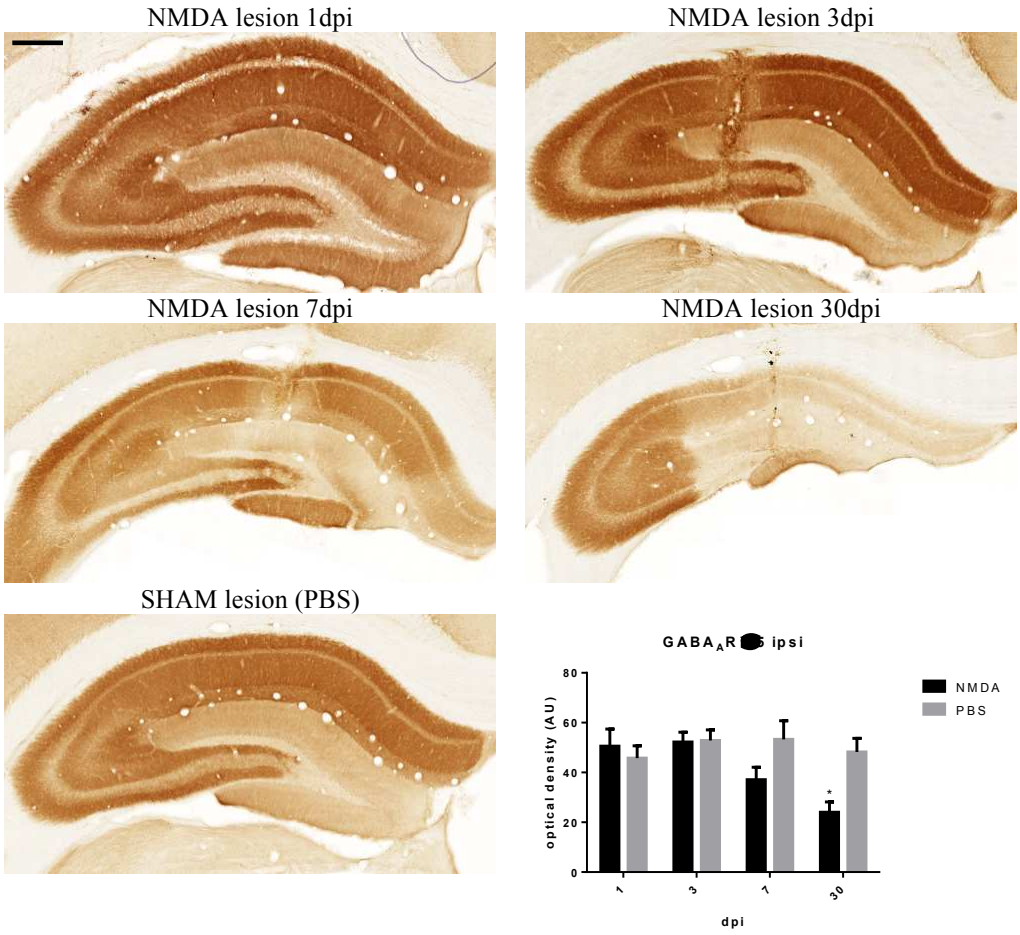

Figure 11: A: Representative images of immunoperoxidase staining using anti-$GABA_A$ receptor α5 subunit antibody taken from the ipsilateral dorsal hippocampus at 1, 3, 7 or 30 days post injection (dpi) of NMDA. We did not observe significant changes in PBS injected hippocampus. NMDA induced progressive loss of α5 subunit expression. The expression was significantly different compare to PBS sham lesion at 30 dpi ($P < 0.05$). Scale bar: A = 500 µm. B: Quantitative analysis of immunoperoxidase staining relative optical density. Values are given as mean ± SEM. * $P < 0.05$.

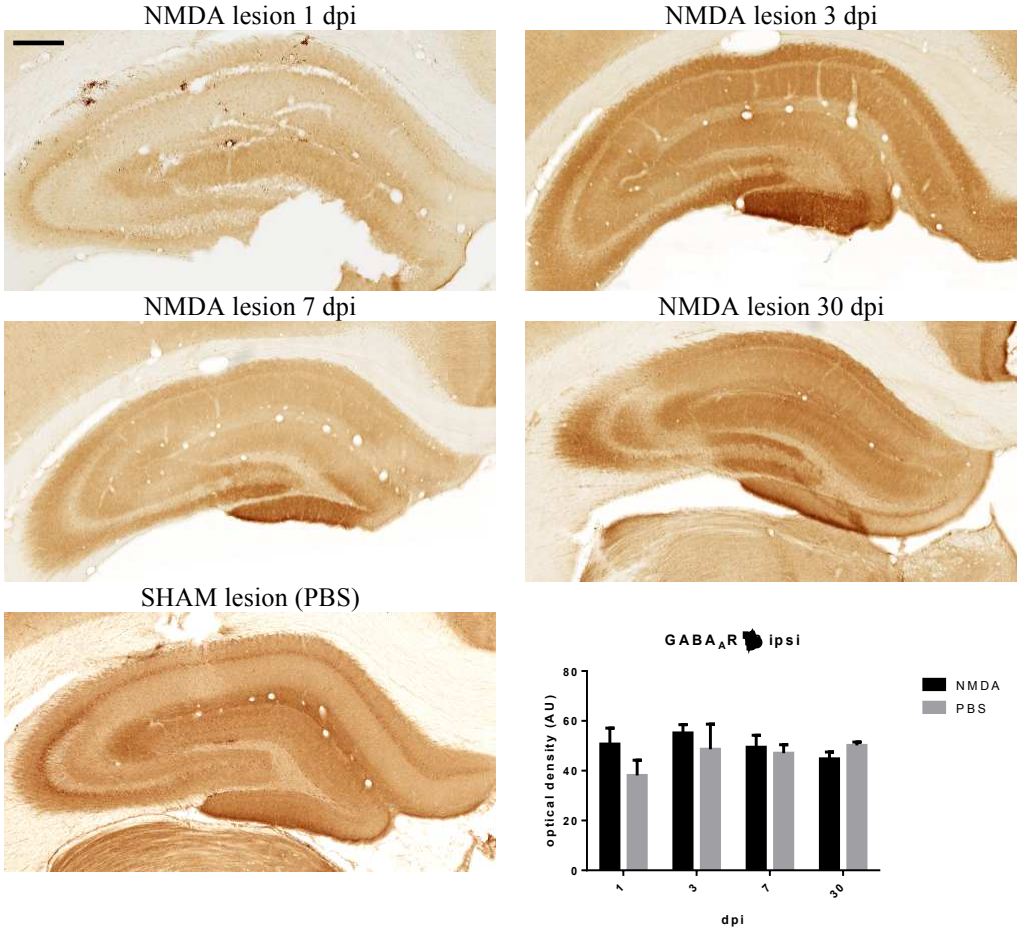

Figure 12: A: Representative images of immunoperoxidase staining using anti-$GABA_A$ receptor γ2 subunit antibody taken from the ipsilateral dorsal hippocampus at 1, 3, 7 or 30 days post injection (dpi) of NMDA. We did not observe significant changes in PBS injected hippocampus. Quantification of relative optical density did not reveal significant changes between NMDA and PBS injected hippocampus ($P > 0.05$). Scale bar: A = 500 µm. B: Quantitative analysis of immunoperoxidase staining relative optical density. Values are given as mean ± SEM.

SUPLEMENTARY

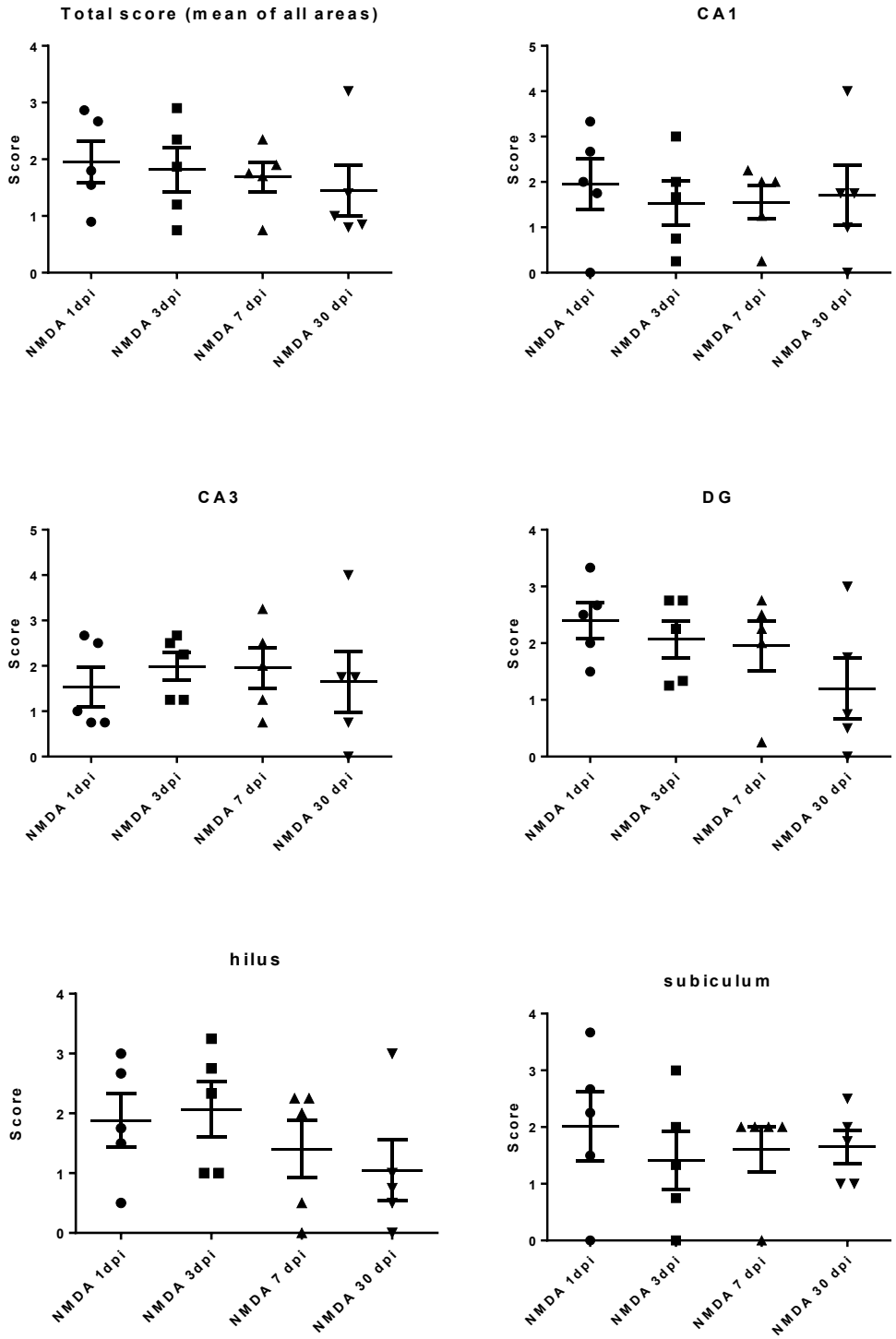

S1: Neural damage score after NMDA lesion of hippocampus 1, 3, 7 and 30 dpi in CA1, CA3, dentate gyrus (DG), hilus and subiculum. No significant differences were observed among individual days post injection. Sham lesion induced no damage (score 0, data not shown) Score scale: 0 – 0-5%, 1 – 6-25%, 2 – 26-50%, 3 – 51-75%, 4 > 75%.

FluoroJade B	Iba-1
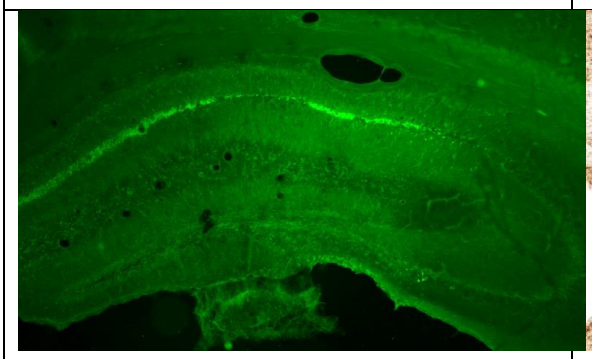	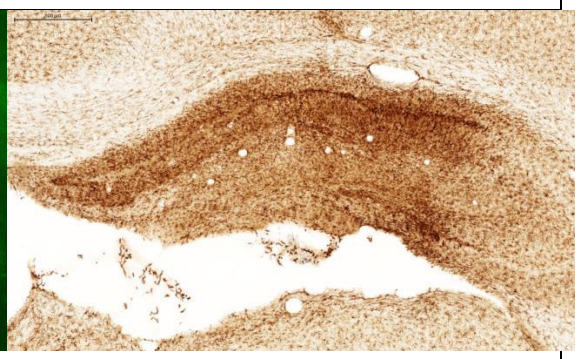
NMDA NR_1	NMDA NR_{2B}
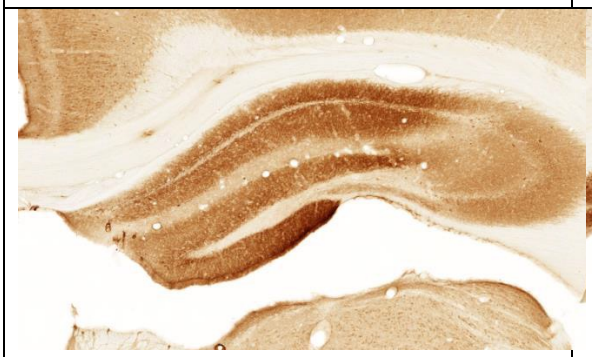	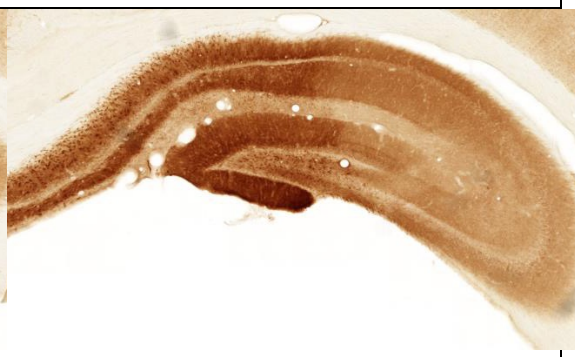
$GABA_A$ α2	$GABA_A$ α5
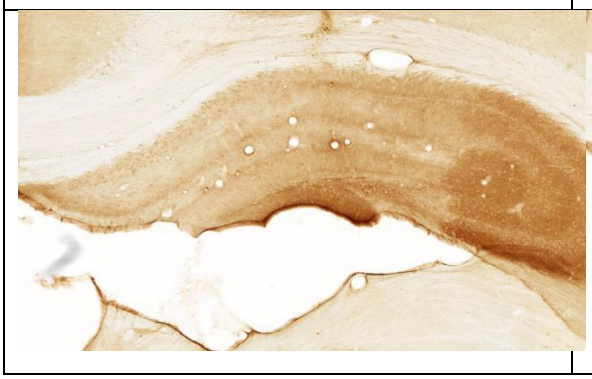	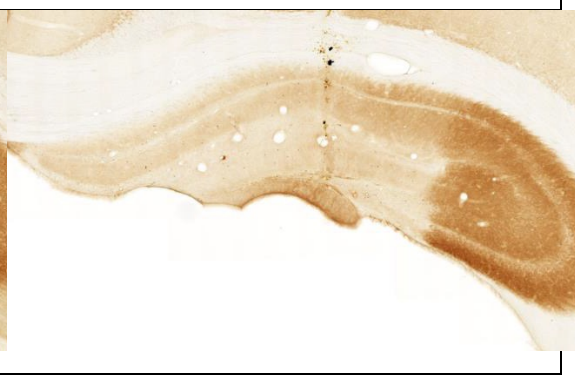

S2: Representative picture of dorsal hippocampus from the same animal demonstrating colocalization of the changes induced by unilateral infusion of NMDA at 30 dpi.

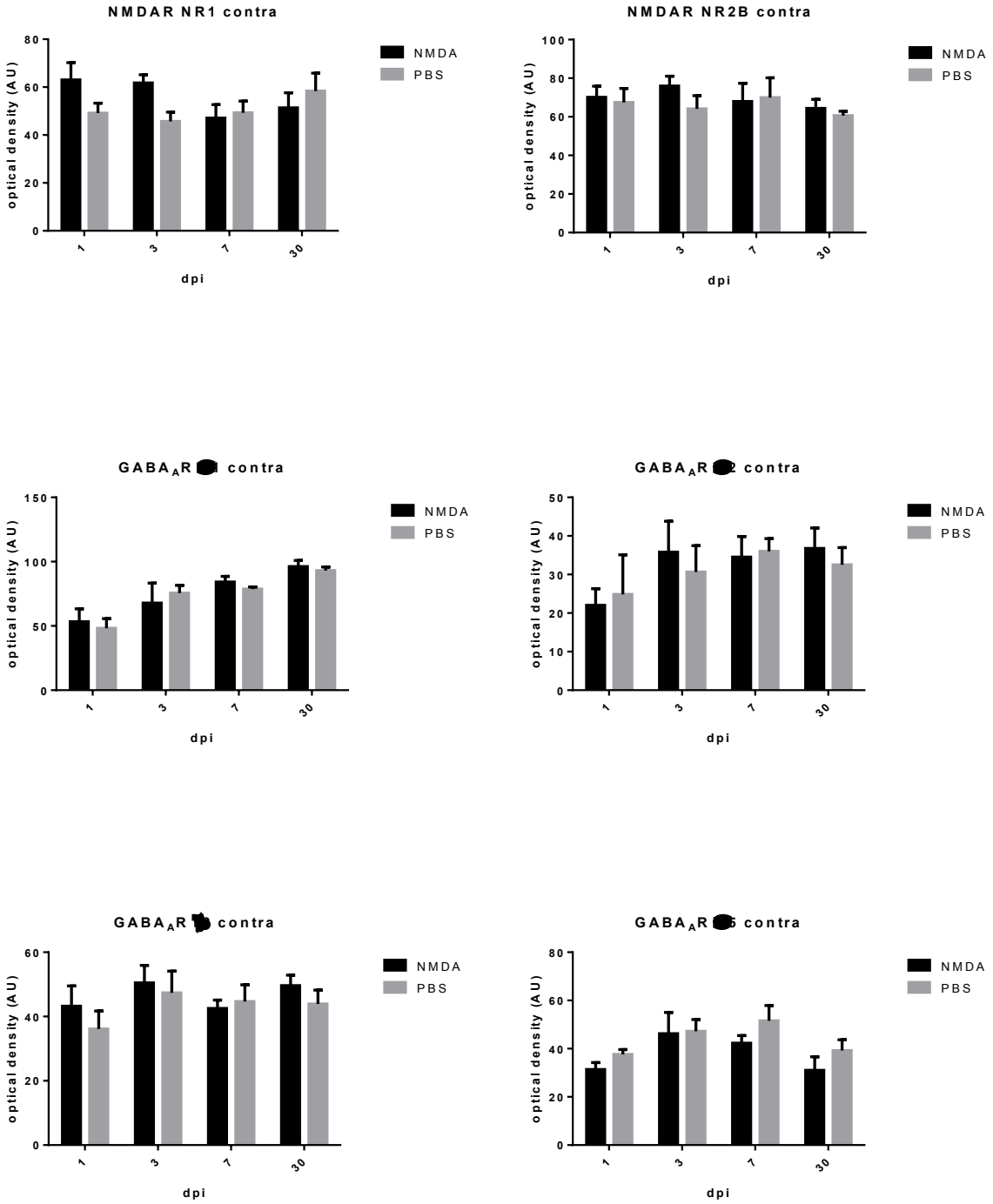

S3: Quantitative analysis of immunoperoxidase staining relative optical density in contralateral (intact) hippocampus. Values for each hippocampus were normalized to neocortex. Statistical analysis did not reveal any difference between NMDA and PBS group ($p < 0.05$). Values are given as mean ± SEM.